Semiconductors, Vol. 38, No. 2, 2004, pp. 125–147. Translated from Fizika i Tekhnika Poluprovodnikov, Vol. 38, No. 2, 2004, pp. 129–150.

REVIEW

Radiation Resistance of SiC and Nuclear-Radiation Detectors Based on SiC Films

A. A. Lebedev, A. M. Ivanov, and N. B. Strokan

Ioffe Physicotechnical Institute, Russian Academy of Sciences, Politekhnicheskaya ul. 26, St. Petersburg, 194021 Russia

e-mail: alexandr.ivanov@pop.ioffe.rssi.ru

Submitted March 5, 2003; accepted for publication April 30, 2003

Abstract—Available results of studying the radiation resistance of SiC and developing the nuclear-radiation detectors based on SiC are analyzed. The data on the ionization energies, capture cross sections, and plausible structure of the centers formed in SiC as a result of irradiation with various particles are reported. The effect of irradiation on the charge-carrier concentration and recombination processes is considered. Two aspects are covered in describing the results of designing SiC-based detectors and studying the detector parameters. First, the specific potential of SiC detectors for solving problems in nuclear physics is considered; typical examples of detector applications are given. Second, the relationship between detector characteristics and the properties of the starting material is considered; a number of methods for determining the specific parameters of SiC based on the characteristics of detectors are described. It is concluded that recent progress in the growth of high-quality SiC films (the difference impurity concentration ranges from 3×10^{14}–3×10^{15} cm^{-3} and the density of micropipe defects is no higher than 1 cm^{-2}) makes it possible to include SiC in the class of materials that can be used to fabricate advanced nuclear detectors. The technological potential of SiC has been far from exhausted; undoubtedly, various configurations of SiC-based detectors (including multielement configurations) will be developed in the near future. © *2004 MAIK "Nauka/Interperiodica".*

1. INTRODUCTION

Modern civilization needs increasingly more consumable-energy sources in order to sustain progress in society. Atomic energy and the solar-radiation conversion using ground-based and orbital converters will probably be the main energy sources in future. Efforts to improve the reliability of both atomic power plants and space-technology systems should be based on the use of radiation-resistant electronics. Radiation resistance typically means that the semiconductor or semiconductor-device parameters are not affected by exposure to nuclear radiation: the higher the radiation dose corresponding to the onset of variation in parameters, the higher the radiation resistance. Semiconductors with a high bonding energy, such as diamond, BN, and SiC, are traditionally thought of as radiation-resistant materials. The advances in technology achieved in the last 10–15 years have made it possible to develop SiC-based devices that have fulfilled the expected high potential of SiC in respect to switching power and high operation temperatures. It is now of current practical interest to check to what extent the radiation resistance of SiC corresponds to theoretical predictions. In this context, the aim of this review is to summarize the available experimental data and assess the correspondence between the parameters of SiC-based devices and theoretical predictions.

In Sections 2 and 3 of this review, we consider both general concepts of radiation resistance of semiconductors as applied to SiC and the properties of radiation defects that appear in SiC as a result of irradiation with gamma-ray photons and various particles. In Section 4, we consider the parameters of nuclear-radiation detectors based on SiC, since these detectors make it possible to compare in the most straightforward way the radiation resistance of materials from which these detectors are manufactured. Nuclear detectors are most sensitive to a large number of properties, including the degradation of parameters of the charge-carrier transport and the emergence of inhomogeneity in these parameters, the temporal stability of the magnitude (and sign) of volume charge of impurities, and the presence of deep-level centers in the case of both capture and generation of charge carriers.

Sections 2 and 3 were written by A.A. Lebedev, and Section 4 was written by N.B. Strokan and A.M. Ivanov.

2. RADIATION DEFECTS FORMED IN SIC EXPOSED TO VARIOUS TYPES OF RADIATION

2.1. Threshold Energy for Defect Production

As mentioned above, the radiation resistance is typically higher for semiconductors with a higher bonding energy. In order to characterize the correlation between

Table 1. Calculated and experimental values of threshold energy for defect production in several semiconductors

Parameter	GaAs	Si	3*C*-SiC	Diamond	6*H*- and 4*H*-SiC
Lattice constant a_0, Å	5.65	5.431	4.36	3.57	3.08
E_d, eV (calculation using (1))	9	12.8	37	80	153
E_d, eV (experiment)	8–20 [2]	13–20 [2]	106 [4]	60–80 [2]	97 [6]
			54–90 [5]		20–35 [7]

the radiation resistance and the bonding energy, the threshold energy for defect production (E_d) is introduced as an important parameter. By this we mean the minimal energy that should be transferred by a particle to the semiconductor atom to form a Frenkel pair (i.e., a vacancy and an interstitial atom) in the lattice [1, 2]. Theoretical calculation of the value of E_d is related to solving the many-body problem and encounters a number of difficulties related to the choice of the type and parameters of the interaction potentials (among other parameters) [2]. When the energy E_d is experimentally determined, the variation in a single chosen parameter under the effect of irradiation is usually monitored, although radiation affects all properties of a semiconductor simultaneously. As a result, the values of E_d exhibit a large spread and depend on experimental conditions. According to Corbett and Bourgoin [3], the quantity E_d and the lattice constant a_0 of a specific semiconductor are related by the following phenomenological formula:

$$1.117E_d = (10/a_0)^{4.363}. \quad (1)$$

Here, E_d is expressed in eV and a_0 is expressed in Å.

The values of E_d calculated using formula (1) for a number of semiconductors and experimental data on E_d are listed in Table 1. As can be seen from Table 1, there is an appreciable spread in the experimental values of E_d for silicon carbide. This spread is possibly related to the low structural quality of SiC crystals, especially those dealt with in studies carried out before the mid-1990s. It is noteworthy that the experimental value of E_d is found to be larger than the values calculated using formula (1) for cubic silicon carbide (3*C*-SiC) and is larger than those for hexagonal silicon carbide (6*H*- and 4*H*-SiC). Since the structural quality of 3*C*-SiC crystals is so far much lower than that of 6*H*- and 4*H*-SiC crystals, we may assume that the value of E_d does not exceed 30–35 eV for all SiC polytypes. This value of E_d is larger than those for Si and GaAs by a factor of 1.5–2 and is smaller than that for diamond by a factor of 2–2.5. However, additional experiments aimed at determining the exact value of E_d and carried out with present-day high-quality epitaxial SiC films are needed. It is also important to determine the temperature dependence of E_d for SiC as a material that is promising for applications in high-temperature electronics.

Table 2. Number of primary radiation defects produced by a single particle or photon in a number of semiconductors; this number was normalized to the corresponding value for silicon carbide

Semiconductor	Protons	Pions	Cosmic rays
Diamond	1.2	0.7	0.5
Silicon	2.4	4.1	3.3
Gallium arsenide	12	43.8	27.5

The values of threshold energies make it possible to calculate the number of primarily produced radiation defects. The data in [8] for materials that are relevant to problems in the physics of high energies (detection of relativistic and cosmic-ray particles) are listed in Table 2. It can be seen that, with respect to the number of primary defects, SiC ranks insignificantly below diamond but is appreciably superior to silicon (and even more so, to gallium arsenide).

2.2. Parameters of Radiation Defects

2.2.1. Irradiation with electrons. Deep levels located at $E_c - 0.35$, $E_c - 0.6$, and $E_c - 1.1$ eV were found in the band gap of *n*-6*H*-SiC irradiated with 3.5- to 4-MeV electrons [9]. The corresponding deep-level centers were annealed out at a temperature of ~1300 K. Taking into account the ionization energies of these centers, the latter can identified with the known structural defects S (E_1/E_2) and Z_1/Z_2 and with the center with a level at $E_c - 1.06$ eV [10]. The research reported in [9] was later continued for *n*-6*H*-SiC irradiated with 2-MeV electrons [11]. In addition to an increase in the background concentration of the E_1/E_2 and Z_1/Z_2 centers, new centers E_3/E_4 ($E_c - 0.57$ eV) were detected. Such an increase in the concentration of the S (E_1/E_2) centers was subsequently observed after irradiation with 2-MeV electrons [12]. In addition, deep-level centers ($E_c - 0.51$ eV) were detected; these centers were annealed out at a temperature of ~1100 K. The *S* centers were found to have the highest thermal stability; they were annealed out at temperatures no lower than ~1300 K.

A number of new deep-level centers were observed in 4*H*-SiC after irradiation of 4*H*-SiC with 2 to 2.5-MeV electrons [12–14], in addition to an increase in the concentration of the background Z_1 centers. These deep-level centers are referred to as EH_1 ($E_c - 0.45$ eV), EH_2 ($E_c - 0.68$ eV), EH_4 ($E_c - 0.72$ eV), EH_5 ($E_c - 1.15$ eV), EH_6/EH_7 ($E_c - 1.65$ eV), and HH_1 ($E_v +$

Table 3. Parameters and properties of radiation defects in 6*H*-SiC

Irradiation with protons [38, 39]			Irradiation with neutrons [24]	Irradiation with electrons [17]	Structural defects	Plausible structure
ionization energy E_t, eV	σ_n, cm^2	annealing temperature, K	ionization energy E_t, eV	the type of defect	the type of defect	
0.16–0.2	6×10^{-17}	800–950	0.13; 0.24	L_1/L_2		A primary defect [39]
0.36/0.4	2×10^{-15}	1100–1800		L_3/L_4	E_1/E_2 [15]; S [40]	A V_{Si} complex [41, 42]
0.5	5×10^{-15}	800–950	0.5	L_6		V_C [17, 42]
0.7	4×10^{-15}	1100–1800		L_7/L_8	Z_1/Z_2 [15]	$V_C + V_{Si}$ [15, 39]
0.8	4×10^{-15}	1100–1800		L_9		
1.1–1.22	2×10^{-15}	1100–1800		L_{10}	R [40]	$V_C + V_{Si}$ [39, 43]

Note: Energy E_t is reckoned from the bottom of the conduction band; σ_n is the cross section for electron capture.

0.35 eV). Many of these centers also appeared after implantation with He and some other ions [15]. Recently [16, 17], it was reported that several new centers had been observed: $E_c - 0.2$ eV, $E_c - 0.32$ eV, and $E_c - 1.34$ eV. The majority of all the aforementioned deep-level centers are also present in unirradiated 4*H*-SiC. The structure of these centers was typically identified with that of defects. Puntilie *et al.* [18] analyzed the effect of the growth conditions of 4*H*-SiC on the concentration of $Z_{1,2}$ centers and suggested that this center was a complex that included a nitrogen atom and an interstitial C atom or, which is less probable, a N atom and a Si vacancy (V_{Si}). The structure of the center with the level at $E_c - 0.5$ eV was also related to that of an impurity–vacancy complex, since this center featured low thermal stability and a low ultimate concentration.

Two types of deep-level centers ($E_v + 0.55$ eV and $E_v + 0.78$ eV) were observed in *p*-6*H*-SiC irradiated with 1.7-MeV electrons [19]. Both types of centers were annealed out at temperatures of 500–800 K. According to the data obtained using the electron spin resonance (ESR) measurements, irradiation of *p*-6*H*-SiC with 300-keV electrons gives rise to Frenkel pairs V_{Si}–Si_I in addition to individual silicon vacancies. Irradiation with 2-MeV electrons gives rise only to monovacancies V_{Si} [20]. Photo-ESR studies of *p*-4*H*-SiC irradiated with 2.5-MeV electrons suggested that the deep-level center ($E_v + 1.47$ eV) could be identified with a positively charged carbon vacancy [21].

2.2.2. Irradiation with neutrons. A number of types of deep-level centers ($E_c - 0.5$ eV, $E_c - 0.24$ eV, and $E_c - 0.13$ eV) were observed in SiC irradiated with neutrons [22–24]. It was assumed [25, 26] that stable vacancy-related complexes were formed as a result of annealing; these complexes were presumably electrically inactive. It was found that weak *n*-type conductivity could be detected in *p*-SiC irradiated with neutrons and not subjected to postirradiation annealing [24, 27]. There were also other publications concerned with the effect of neutron radiation on the properties of SiC [28, 29]. The effect of neutron radiation on the current–voltage characteristics of various devices has been studied in most detail. It has been established that the carrier-removal rate (the number of removed carriers per one neutron and one centimeter) amounts to ~4.5 cm^{-1}, which is lower than that in silicon by a factor of approximately 3 [30]. The centers with a deep level at $E_c - 0.49$ eV were detected in 3*C*-SiC irradiated with neutrons; these centers were annealed out at a temperature of ~650 K [31]. The measured carrier-removal rate is equal to 7.2 cm^{-1}, which is close to the value of 7.8 cm^{-1} measured for silicon irradiated with neutrons with the identical spectrum. Two annealing stages (at 350 and 500 K) were observed in studies of the charge-carrier mobility in *n*-SiC irradiated with reactor neutrons [32].

2.2.3. Irradiation with alpha particles. It was reported [33] that irradiation of *n*- and *p*-6*H*-SiC with alpha particles only brought about an increase in the concentration of already existing background defects. It was concluded that the radiation resistance of SiC is no lower than the radiation resistance of InP, which is another radiation-resistant material. The effect of irradiation with He^+ ions on 4*H*- and 6*H*-SiC was considered in detail by Dalibor *et al.* [15]. The parameters of observed radiation defects coincided to a large extent with those of radiation defects detected previously in SiC irradiated with electrons.

2.2.4. Irradiation with gamma-ray photons. The results of studying the ESR spectra of *p*-4*H*- and *p*-6*H*-SiC crystals irradiated with gamma-ray photons were reported by Il'in *et al.* [34]. Three types of paramagnetic centers were detected; these centers decomposed at 160°C. It was assumed that the corresponding ESR spectrum was related to a single type of centers that involved carbon vacancies or to a complex composed of an Al impurity atom and a C atom that occupies the silicon or interstitial sites.

2.2.5. Irradiation with protons. Deep-level centers formed in 4*H*- and 6*H*-SiC of *n*-type conductivity as a result of irradiation with 8-MeV protons were previ-

Table 4. Parameters and properties of radiation defects in 4*H*-SiC

Irradiation with photons [39]			Irradiation with electrons [12–14, 16, 17]	Implantation of He^+ [15]	Structural defects	Plausible structure
ionization energy E_t, eV	σ_n, cm^2	annealing temperature, K	ionization energy, defect type	the type of defect	ionization energy, defect type	
0.18	6×10^{-15}	800–950	$E_c - 0.2$ eV	P_1/P_2	$E_c - (0.18–0.2)$ eV [44]	A primary defect [39]
			EH_1 ($E_c - 0.45$ eV)			Vacancy + impurity [16]
0.63–0.7	5×10^{-15}	1100–1800	EH_2, EH_4	Z_1	Z_1 [15]	V_C [39], a V_{Si} complex [45] N + V_{Si}, [18]
0.96	5×10^{-15}	1100–1800		$RD_{1/2}$	$E_c - 1.1$ eV [46]	$V_C + V_{Si}$ [39, 47]
1.0	1×10^{-16}	1100–1800	EH_5	RD_3		
1.5	2×10^{-13}	1100–1800	EH_6/EH_7	RD_4		

Note: Energy E_t is reckoned from the bottom of the conduction band; σ_n is the cross section for electron capture.

ously studied in detail [33–37]. The parameters of these centers are close to those of the centers detected previously in SiC irradiated with electrons (Tables 3, 4). The ESR data show that the observed centers are either carbon vacancies ($E_c - 0.5$ eV in 6*H*-SiC and $E_c - (0.63–0.7)$ eV in 4*H*-SiC) or pairs of vacancies in the carbon or silicon sublattices. Apparently, the different thermal-ionization energies of centers that presumably have the same structure ($V_{Si} + V_C$) can be attributed to dissimilar distances between the components of the pairs (vacancies); these distances are characteristic of each of the aforementioned radiation defects. The above results were obtained using the method of positron spectroscopy for *n*-6*H*-SiC irradiated with low-energy protons [43, 48]. It was found that irradiation with protons gave rise to various types of divacancies $V_{Si} + V_C$, as well as individual vacancies that were annealed out at a temperature of ~900°C [48]. It was also assumed that a certain divacancy was responsible for a center with a deep level near the midgap [43]. At the same time, only silicon monovacancies annealed out at a temperature of ~1100°C were observed in the *n*-6*H*- and *n*-4*H*-SiC samples irradiated with 12-MeV protons [49]. Davydov *et al.* [50] analyzed the results of studying *n*-6*H*-SiC irradiated with protons with various energies. It was shown that the *R* centers ($E_c - 1.1$ eV) featured the highest production rate: 0.17, 70, and 700 cm^{-1} for protons with energies of 1 GeV, 8 MeV, and 150 keV, respectively.

2.3. Defect-Related Luminescence

Short-wavelength luminescence with photon-emission energies ranging from 2.3 to 2.6 eV in *n*-6*H*-SiC crystals irradiated with K and Li ions and then annealed was first observed by V.V. Makarov in 1966 [51]. The luminescence spectrum consisted of (i) two triplets of narrow lines (*H* and *L* lines) near an energy of 2.6 eV and (ii) a broad featureless band with an emission peak at 2.35 eV. It was ascertained [52, 53] that the broad band did not result from the development of a fine structure. It was assumed that this band was related to radiative recombination involving a donor nitrogen level and an acceptor center that was produced in the course of implantation. Patrick and Choyke [54] studied in detail the structure of the *H* and *L* lines and the temperature dependences of the luminescence spectrum; the latter was called the D_1 spectrum. This spectrum was observed in SiC after irradiation with electrons [55], neutrons [56], and ions of various types [53], which made it possible to use 6*H*-SiC ion-implanted with Al as a material for fabricating efficient light-emitting diodes that operated in the green region of the spectrum [57]. Irradiation of other SiC polytypes gave rise to luminescence with similar properties [52]. Since this luminescence emerged as a result of irradiation or implantation of SiC with various ions, it was assumed that a center acting as the activator of luminescence had either a pure defect-related structure or was a complex which consisted of an intrinsic defect and an atom of a background impurity [58–60]. Choyke [61] detected excitons bound to deep-level centers in SiC. However, the levels related to these centers were not observed. It was assumed that the D_1 spectrum could be related to the Z_1 centers in 4*H*-SiC [15] or to the *i* centers in 6*H*-SiC [62].

It may be concluded from the consideration of the summarized results of studying the radiation defects in SiC that the spectrum of radiation defects in each of the silicon carbide polytypes is almost independent of the methods for growing the samples and the type of particles used for irradiation (protons, electrons, alpha particles). In addition, irradiation mainly brings about an increase in the concentration of deep-level centers that already exist in the material. According to ESR data, the vast majority of radiation defects consist of elementary lattice defects, i.e., vacancies and interstitial atoms

Table 5. Values of V_d for SiC and Si according to various publications

Semiconductor	$N_d^+ - N_a^-$, cm^{-3}	Particles/energy/dose	V_d, cm^{-1}	References
4*H*-SiC	1×10^{15}	α/1.7 MeV/2×10^9 cm^{-2}	4×10^5	[65, 66]
	2×10^{18}	H^+/350 keV/1×10^{14} cm^{-2}	2×10^4	[67]
		Protons/8 MeV/6×10^{14} cm^{-2}	130	[39]
		The same	67*	[39]
6*H*-SiC		α/55 MeV/2×10^{11} cm^{-2}	7.8×10^4	[33]
		Neutrons	4.5	[69]
	4×10^{16}	Protons/8 MeV/6×10^{14} cm^{-2}	17	[39]
	The same	The same	–45*	[39]
3*C*-SiC	10^{16}	Neutrons/1 MeV/10^{14} cm^{-2}	7.2	[68]
		Electrons/1 MeV	0.014	[70]
Si		α/1.7 MeV/2×10^9 cm^{-2}	5×10^4	[65, 66]
		Neutrons/1 MeV/10^{14} cm^{-2}	7.8	[68]
		Electrons/1 MeV	0.01–0.1	[2]
		Protons/8 MeV/6×10^{14} cm^{-2}	200–350	[71, 72]

* T = 650 K. Other quantities were measured at T = 300 K.

(or their combinations). Irradiation of SiC was carried out at temperatures of 295 K or lower in all the studies cited above. Apparently, primary radiation defects in SiC at the aforementioned temperatures have a low mobility and cannot form complex secondary defects that include, for example, impurity atoms.

3. EFFECT OF RADIATION ON MATERIAL PROPERTIES

3.1. The Lifetime of Minority Charge Carriers

It is known that radiation is used to reduce the lifetime of charge carriers in fast-response devices based on Si. Such a method for reducing the lifetime has practically not been employed in the case of SiC, since the problem of increasing the lifetime of minority charge carriers is more urgent for this material. Nevertheless, this problem may arise in future. At present, there is no generally accepted opinion as to which deep-level centers control the lifetime in SiC. For 6*H*-SiC, it was shown that the *R* centers with the level at $E_c - 1.1$ eV (near the midgap of this polytype) can act as the aforementioned lifetime-controlling centers [63]. Lebedev *et al.* [37] measured the hole diffusion length (L_p) in *n*-6*H*-SiC irradiated with various doses of 8-MeV protons. Figure 1 shows the dependence of L_p^2 on the concentration of *R* centers (N_R). As can be seen from Fig. 1, the dependence $L_p^2 \propto 1/N_R$ is the same for irradiated samples as for unirradiated samples. Thus, the radiation-based method for controlling the lifetime may turn out to be promising in *n*-6*H*-SiC where the production rate of *R* centers exceeds that of other radiation defects.

3.2. The Rate of Removal of Charge Carriers in Silicon Carbide

The formation of radiation defects with deep levels in the band gap of a semiconductor brings about a redistribution of charge carriers and a change in the conductivity of the material. If a material with *n*-type conductivity is irradiated, electrons are transferred from the

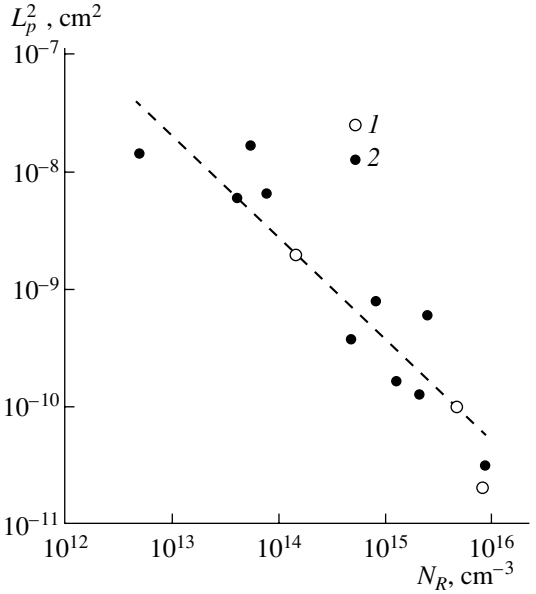

Fig. 1. Dependence of the hole diffusion length on the concentration of the *R* centers [37]. Unfilled circles *1* correspond to the sample after irradiation with several doses and annealing; filled circles *2* correspond to an unirradiated samples.

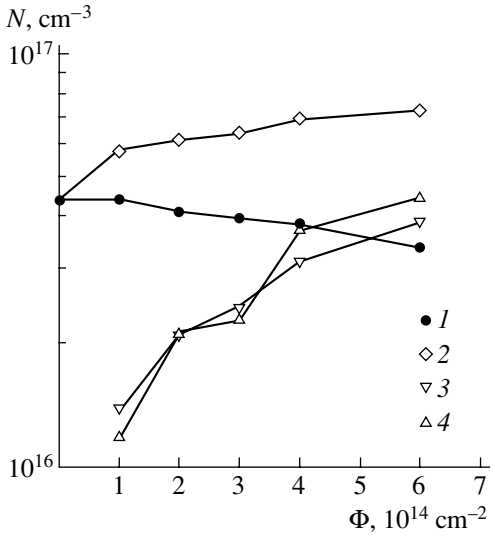

Fig. 2. Dependences of characteristic concentrations N in 6*H*-SiC on the dose of irradiation with protons [39]. Curves *1* and *2* correspond to $N_d^+ - N_a^-$ at $T = (1)$ 300 and (*2*) 650 K; curve *3* represents the difference between curves *2* and *1*; and curve *4* represents the concentration of the centers with the level at $E_c - (1.1–1.22)$ eV.

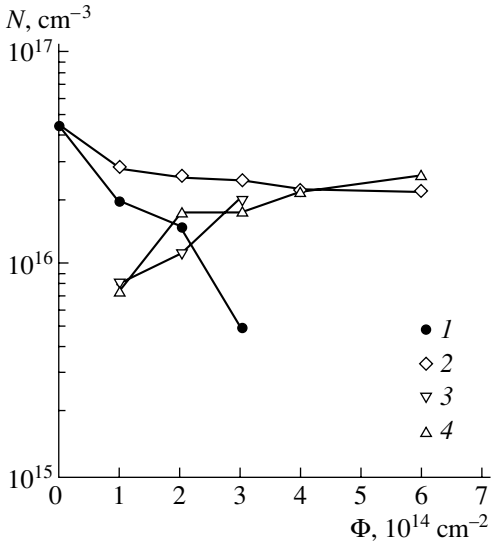

Fig. 3. Dependences of characteristic concentrations N in 4*H*-SiC on the dose of irradiation with protons [39]. Curves *1* and *2* correspond to $N_d^+ - N_a^-$ at $T = (1)$ 300 and (*2*) 650 K; curve *3* represents the difference between curves *2* and *1*; and curve *4* represents the total concentration of radiation defects $RD_{1,2} + RD_3 + RD_4$.

conduction band to deep levels of acceptor-type radiation defects.

As a result, the conductivity of the material decreases, so that the semiconductor can become an insulator if the radiation doses are high. In order to describe this process in various materials, the removal rate for charge carriers V_d is used; this parameter is defined as

$$V_d = \Delta n/\Phi = (n_0 - n)/\Phi, \qquad (2)$$

where n_0 and n are the concentrations of charge carriers in the conduction band before and after irradiation and Φ is the radiation dose. Lebedev *et al.* [64] considered the special features of determining the parameter V_d for silicon carbide and wide-gap semiconductors (WGSs) in general. Deep-level centers with an ionization energy of $\gtrsim 1$ eV can be formed in irradiated semiconductors with a wide band gap E_g. Such centers will virtually not be ionized at room temperature, and the quantity V_d will exhibit a temperature dependence that will become less pronounced with increasing temperature of measurements even at temperatures higher than 295 K.

We now consider experimental studies in which the quantity V_d was determined when SiC was irradiated with particles of various types. The results of these studies and the available values of V_d for silicon obtained under the same irradiation conditions are listed in Table 5.

According to the data obtained in the majority of studies, $V_d(\mathrm{Si}) \geq V_d(\mathrm{SiC})$ at 300 K. Data obtained recently [65, 66] contradict the general pattern: $V_d(\mathrm{SiC})/V_d(\mathrm{Si}) \sim 10$. Crystals were irradiated with 1.7-MeV alpha particles with a dose of 2×10^9 cm^{-2} [65, 66]. The ion ranges were equal to 3.8 μm for SiC and 5.9 μm for Si. It is worth noting that only the effects at the end of the particle ranges were monitored in [65, 66]; therefore, the effect could be attributed mainly to helium clusters formed at this depth rather than to radiation defects.

In addition, the results reported so far [65–70] were obtained at room temperature, in which case the value of V_d is still large. The deep-level centers formed in *n*-4*H*- and *n*-6*H*-SiC as a result of irradiation with 8-MeV protons were studied in [35–39]. It was established that the difference concentration of ionized donors and acceptors $N_d^+ - N_a^-$ measured at room temperature decreased after irradiation. At the same time, it was observed that this concentration increased after heating the structure to 650 K. The value of $N_d^+ - N_a^-$ measured at 650 K in irradiated 6*H*-SiC was even larger than in unirradiated samples. As the radiation dose increased, this difference between the irradiated and unirradiated samples increased (Figs. 2, 3). Thus, the measurements performed at high temperatures support the conclusion that for SiC either $V_d(300\ \mathrm{K}) > V_d(650\ \mathrm{K})$ (for 4*H*-SiC) or the value of V_d (650 K) becomes negative (for 6*H*-SiC) [39]. Evidently, both donor and acceptor radiation defects (with donors being dominant) are formed as a result of irradiation of *n*-6*H*-SiC. Apparently, the same mechanism is also active for *p*-6*H*-SiC, in which case the change in the conductivity type ($p \longrightarrow n$) is observed as a result of irradiation [39].

An approach to the formation of radiation defects in WGSs was previously developed [73] in which a mechanism similar to the self-compensation of conductivity was considered. According to Vinetskiĭ and Smirnov [73], the change in the conductivity type as a result of irradiation is characteristic only of narrow-gap semiconductors, whereas the conductivity of WGSs tends to intrinsic conductivity as the radiation dose increases. Indeed, this inference is consistent with experiment only if the irradiation of WGSs is carried out at room temperature. However, if the temperature dependence of V_d is taken into account, the aforementioned approach is valid only for 4*H*-SiC. An increase in the difference concentration of donors and acceptors $N_d^+ - N_a^-$ as a result of irradiation is observed in 6*H*-SiC and, apparently, in 3*C*-SiC [74].

Thus, measurements of V_d at room temperature cannot clarify whether the devices based on WGSs are suitable for operation at high temperatures.

3.3. Radiation-Induced Doping (Compensation) of SiC

Another important aspect of the interaction of ionizing radiation with semiconductors is the phenomenon of radiation-induced doping. As a result of this doping, local regions with the high resistivity required for fabricating a specific device can be formed in a semiconductor. It is generally believed that the radiation resistance and the feasibility of radiation-induced doping are contradictory characteristics of a material; i.e., if a semiconductor is radiation-resistant, this material is considered as not suitable for compensation by the method of radiation-induced doping.

In what follows, we will show that the above assessment is not quite correct in the case of SiC. It is known that SiC is a promising material not only in relation to high-temperature electronics but also with respect to applications in a number of devices that are not designed for operation at high temperatures. These devices primarily include high-frequency devices (Schottky diodes and certain types of field-effect transistors) whose structure involves a metal–semiconductor contact. As a rule, such a contact degrades rapidly with increasing temperature, irrespective of the limiting operation temperatures of the semiconductor itself. If the operation temperatures of the device are not much higher than 300 K, we can use the values of V_d obtained at 300 K in order to estimate the efficiency of radiation-induced doping of SiC. The largest value of resistivity (ρ_M) that can be attained in the semiconductor is another important characteristic of the efficiency of radiation-induced doping.

As a result of irradiation, the Fermi level in an *n*-type material should shift to the deepest level of the radiation defects produced. The value of ρ_M should be controlled by the concentration of charge carriers in the conduction band of a semiconductor, i.e., by the level depth and degree of ionization of a given deep-level center. If the semiconductor's band gap becomes wider, radiation defects with deeper levels and with a lesser degree of ionization can be formed in this semiconductor. Thus, WGSs offer clear advantages over narrow-gap semiconductors in the production of high-resistivity layers. It is important that the semi-insulating properties of these layers are also retained at temperatures higher than 295 K. As shown by Anikin *et al.* [63], the resistivity of 4*H*-SiC at T = 450°C is equal to the largest value attained for GaAs (~10^9 Ω cm) at room temperature.

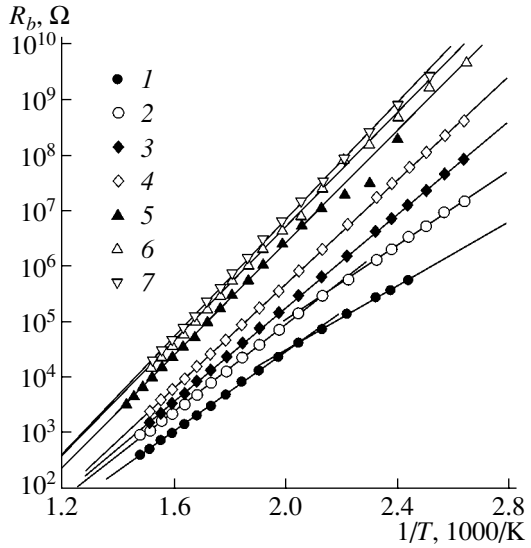

Fig. 4. Temperature dependences of the forward resistance of a Schottky diode based on 6*H*-SiC after proton irradiation with doses Φ = (*1*) 3×10^{14}, (*2*) 4×10^{14}, (*3*) 6×10^{14}, (*4*) 1×10^{15}, (*5*) 2×10^{15}, (*6*) 5×10^{15}, and (*7*) 1×10^{16} cm^{-2}.

A number of researchers have studied the feasibility of proton (hydrogen) passivation of silicon carbide [67, 75–78]. It was shown that the resistivity of *n*-4*H*-SiC at room temperature exceeded 8×10^6 Ω cm after irradiation with 350-keV protons with a dose of 1×10^{14} cm^{-2} [67]; the resistivity decreased rapidly with increasing temperature. Irradiation with 8-MeV protons [39] also brought about an increase in the ohmic resistance of 4*H*- and 6*H*-SiC structures subjected to forward biases (R_b) at room temperature. In contrast to 6*H*-SiC, a decrease (rather than an increase) in total concentration of uncompensated donor centers is observed in 4*H*-SiC samples irradiated with protons. This observation shows that irradiation stimulates the formation of acceptor centers with levels in the lower half of the band gap or the destruction of donor centers with levels in the upper half of the band gap. In addition, irradiation gives rise to acceptor centers with deep levels to which electrons transfer from shallower donor levels.

According to data published [39], the value of R_b decreased exponentially with increasing temperature and featured activation energy ε_A (Figs. 4, 5). As the radiation dose increased, the energy ε_A became higher and tended asymptotically to ~1.1 eV for 6*H*-SiC and

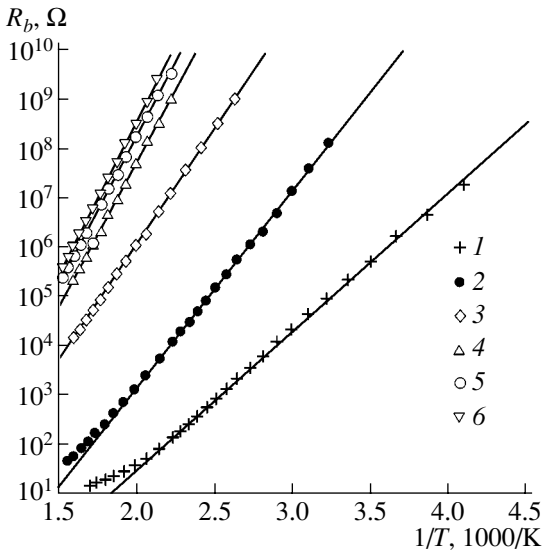

Fig. 5. Temperature dependences of the forward resistance of a Schottky diode based on 4*H*-SiC after proton irradiation with doses Φ = (*1*) 6×10^{14}, (*2*) 1×10^{15}, (*3*) 2×10^{15}, (*4*) 5×10^{15}, (*5*) 1×10^{16}, and (*6*) 2×10^{16} cm^{-2}.

1.25 eV for 4*H*-SiC [39]. This behavior resulted in the formation of *n*-6*H*-SiC layers that were semi-insulating at room temperature. Such layers can be used in the fabrication of devices that are not designed for operation at high temperatures, for example, photodetectors or various radiation detectors.

3.4. Amorphization of SiC as a Result of Irradiation

Amorphization of SiC samples was observed after irradiation with electrons [79], neutrons [80], protons, and various ions (He, Ar, Cr) [81]. It was also noted [81] that the process of amorphization in SiC differed from that characteristic of Si. Only ions that are heavier than B can amorphize silicon at room temperature; lighter ions only give rise to heavily damaged layers of crystalline material even at high implantation doses. At the same time, amorphization of SiC sets in if the critical specific implantation energy (23 eV/atom) is attained, irrespective of the ion mass. It was noted [81] that this difference between Si and SiC may be related to a higher mobility of defects in silicon at room temperature and to the partial annealing (recombination) of these defects directly within the ion track during implantation.

It was also observed [79, 80] that annealing of amorphized layers of hexagonal SiC polytypes led not only to the recovery of the starting-polytype structure but also to the formation of inclusions of the cubic polytype 3*C*-SiC. In our opinion, these results are very important since the physical theory of mutual transformations of SiC polytypes is far from adequate. We believe that it is especially important to gain insight into the causes of changes in the polytype in an already grown epitaxial layer or a device structure. Recently, there have been a number of publications concerned with studies of stacking faults that consisted of inclusions of cubic SiC within diodes based on 4*H*- or 6*H*-SiC. These inclusions were formed when forward current flowed through the diodes under consideration [82–84].

The effect of the above inclusions is usually considered as detrimental since stacking faults represent the regions of efficient recombination of charge carriers and the formation of these regions results in the degradation of parameters of high-power devices based on silicon carbide. At the same time, it was shown that stacking faults with a thickness on the order of several lattice constants act as 3*C*-SiC quantum wells within the wider-gap 4*H*-SiC. As a result of dimensional quantization, the above circumstance resulted in the appearance of intense photoluminescence in the blue region of the spectrum (photon energy $h\nu = 2.5$ eV) [85]. It was also observed that quantum-dimensional stacking-fault structures were formed in a heavily doped 4*H*-SiC layer after additional heat treatment [86]. Unfortunately, the process of formation of stacking faults and related quantum wells in SiC is hitherto uncontrollable.

Even before the first studies of stacking faults, it was inferred from an analysis of the properties and structure of deep-level centers in silicon carbide that intrinsic-defect concentration characteristics existed for each polytype [10, 87]. A variation in the intrinsic-defect concentration can then lead to transformation of a polytype. It was assumed that irradiation (possibly, up to the onset of amorphization) with subsequent annealing can be used to change the defect concentration in a grown structure.

The development of the technology described above would make it possible to radically expand the range of SiC applications and affect the studies of other polytype compounds. However, this method of forming heterostructures requires extensive studies of the irradiation and annealing conditions and preliminary doping of the starting epitaxial layers in order to prove its feasibility.

The formation of hydrogen or helium bubbles in the case of high implantation doses with subsequent exfoliation of the top semiconductor layer in the course of annealing is one of the difficulties in carrying out the aforementioned studies [88, 89]. At the same time, significant progress has been achieved in recent years in the fabrication of heteropolytype SiC structures using epitaxial methods [90–92].

4. THE USE OF SiC FOR DETECTION OF NUCLEAR RADIATION

4.1. History

Nuclear detectors based on SiC occupied a prominent place among detectors even in the first attempts in the 1960s to replace a gas in ionization chambers with a more condensed (semiconductor) medium.

It should be recalled that the typical design of a detector (by analogy with a gas-filled chamber) includes a p^+–n- (n^+–p-) or p^+–i–n^+ diode structure. This structure operates under conditions of reverse bias, which forms an operation (active) zone, i.e., a space-charge region (SCR) with a strong electric field. The p^+- and n^+-type regions act as electrodes. Nuclear particles (or photons) produce ionization in a semiconductor when they are slowed down. Thus, the tracks of nonequilibrium electron–hole pairs are formed in the detector's operation volume. The separation of charge carriers in an electric field of SCR and their subsequent drift to electrodes generate a current pulse in the detection circuit.

Ionization occurs with relatively small fluctuations in the number of generated electron–hole pairs; as a result, this number is found to be strictly related to the absorbed energy. Therefore, in the case of complete transfer of charge carriers to electrodes, the charge that flows through the circuit represents a measure of the absorbed particle (photon) energy.

In order to successfully implement the "ionization" principle of measuring the energy of nuclear radiation, the starting material should feature a certain set of properties. These properties include a low concentration of impurities (an extended region of the electric field); bipolar conductivity (the absence of a space-charge accumulation that distorts the electric field); large drift length for charge carriers (charge-carrier transport with an efficiency close to unity); a band gap ensuring the low-rate thermal generation of charge carriers (a low noise and a low dissipated power); and, if possible, a large atomic number of relevant elements (efficient absorption of the X- and gamma-ray radiation). Since the ion tracks occupy a small fraction of the detector volume, a high local uniformity of conditions of the charge-carrier transport is required for the pulses to be identical.

Unfortunately, the improvement rate for the SiC properties in the 1960s–1970s was appreciably lower than that for competing materials. For example, perfect monatomic Ge and Si crystals were rapidly obtained and methods for high-degree compensation of residual p-type conductivity using the donor lithium impurity were developed. At the same time, materials with a wider band gap and larger atomic number than those for Ge and Si (CdTe and CdZnTe solid solutions, the compounds GaAs and HgI_2) were developed. The aforementioned materials were found to be very efficient in the spectroscopy and detection of various types of nuclear radiation. The advantages of planar technology were exploited, and various designs of silicon detectors (including multielement detectors) became widely implemented. As a result, interest in SiC as a material for detectors was temporarily reduced, although the first results of using SiC to fabricate nuclear detectors were encouraging [93–95].

The successful attempt of Tikhomirova *et al.* [96–98] to introduce a beryllium acceptor impurity into n-type crystals should be mentioned among studies concerned with SiC that were carried out in the 1970s. Detectors with n-type conductivity compensated with beryllium operated with good results as counters of neutrons (conversion reactions with emission of short-range particles were used) and fission fragments directly in the reactor channel; these counters could operate at temperatures as high as 600°C.

Considerable advances have been made recently in controlling the properties of SiC: the requirements imposed on most important characteristics of SiC are now satisfied quite adequately. Consequently, a renewed interest in designing SiC-based detectors is clearly observed. In what follows, we will do our best to describe the current situation in this field.

The difference concentration of donors and acceptors $N_d^+ - N_a^- = 5 \times 10^{14}$–$3 \times 10^{15}$ cm^{-3} is standard for "pure" SiC films. This concentration makes it possible to obtain an SCR with extent $W \approx 15$–30 μm at a bias voltage $U = 500$ V. Lifetimes on the order of several hundreds of nanoseconds for holes with lower mobility combined with large values of saturation drift velocity ensure an almost 100% efficiency of the charge transport. As mentioned above, the high radiation resistance and chemical resistance of SiC and its high thermal stability (SiC-based devices can operate at temperatures of several hundreds of degrees centigrade) are the most attractive characteristics of SiC. Much attention in recent publications has been given to studying the above properties of SiC and to tests of SiC-based detectors for detection and spectrometry of various types of nuclear radiation.

In turn, the diode structures of detectors are convenient for studying the electrical characteristics of the material. In this context, deep-level transient spectroscopy (DLTS) and electron-beam-induced current (EBIC) are widely used. The main method for determining the transport characteristics is the amplitude analysis of transport of calibrated bunches of nonequilibrium charge carriers.

4.2. Detection of Short-Range Particles

The majority of studies concerned with analyzing the operation of SiC detectors have been carried out using epitaxial n-4H- or n-6H-SiC films with $N_d^+ - N_a^- = 10^{15}$ cm^{-3}. The film thickness was equal to ~10 μm, i.e., was comparable with the slowing-down length of short-range ions. Single-crystal SiC wafers that were doped to the level of $(3.0$–$6.0) \times 10^{18}$ cm^{-3} and had a thickness of ~300 μm were used as the substrates. As a rule, the rectifying contact was prepared in the form of a Schottky barrier. The latter was formed using magnetron sputtering of Ni [99, 100] or by depositing a thin (100 nm) Au film [101].

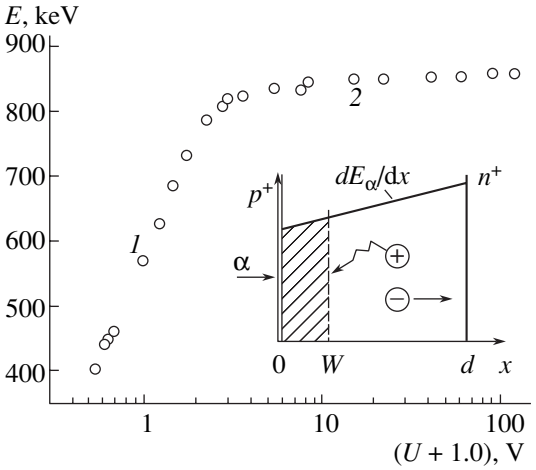

Fig. 6. Amplitude of the signal corresponding to alpha particles (energy E measured by instrumentation) as a function of the voltage applied to the detector's diode structure (see [99]). Circles *1* corresponds to the structure before depletion, and circles *2* corresponds to complete depletion. The inset illustrates the configuration used in the analysis of diffusion; the quantity W corresponds to the SCR boundary; and E_α stands for the energy of incident alpha particles.

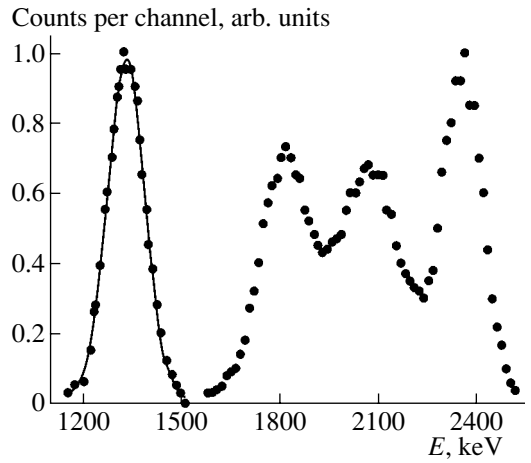

Fig. 7. Alpha-particle energy spectrum obtained using an n–p–n^+ structure based on a 4*H*-SiC film. The solid line represents the approximation of the low-energy line using a Gaussian function at the relative full width at the half-maximum of the line FWHM = 8.6%.

It is convenient to use natural-radioactivity alpha particles with energies of 5–6 MeV as a highly ionizing radiation. The detection of nonequilibrium charge induced by individual alpha particles is performed using standard nuclear spectrometry instrumentation. This instrumentation includes a charge-sensitive preamplifier, an amplifier with the passband controlled by integrating/differentiating *RC* circuits, and a pulse-height analyzer. In order to calibrate the energy width of an analyzer channel, a precision silicon detector is used. The spectrum shape and the average amplitude and full width of the spectrum at half-maximum were determined in the studies under consideration.

The typical dependence of the signal amplitude (energy E dissipated in the film) on the bias voltage applied to the detector is shown in Fig. 6 for a film with thickness $d \approx 10$ μm [99]. ^{244}Cm alpha particles with range $R \sim 20$ μm were used; i.e., the particle range exceeded the film thickness, so that the induced ionization virtually corresponded to the linear portion of the Bragg curve for specific energy losses $dE_\alpha/dx = f(x)$. The observed two stages in the signal growth correspond to voltages U before and after complete depletion of the structure. As long as the SCR occupies only a fraction of the n-type base volume, the diffusion of holes in the base is involved in the charge transport in addition to the drift of charge carriers in the field region; the diffusion proceeds much more slowly than the drift. Appreciable losses of charge due charge-carrier recombination become significant. In the first approximation, the signal increases in proportion to the SCR width $W \propto U^{1/2}$ (a similar result was reported by Nava *et al.* [101].

When the SCR occupies the entire film thickness, electrons and holes are efficiently separated by the field and the losses of charge are controlled by localization at the capture centers that retain the charge carriers for a time that exceeds the pulse-shaping time in the detecting instrumentation (on the order of several microseconds). The signal increases insignificantly owing to an increase in the drift velocity. Finally, the charge transport is assumed to be complete at the stage of signal saturation.

The shape of the spectral line was found to be Gaussian [99, 101]; an appreciable transformation of the line as the average value of the amplitude increased was not observed (see 4.3.3 below).

Figure 7 illustrates the feasibility of detecting a spectrum that consists of four lines of the ^{226}Ra alpha decay. The decay energies were reduced owing to a slowing-down of alpha particles in air and were equal to 2432, 3469, 4125, and 6189 keV. The ranges of all the particles were smaller than the film thickness; however, the charge transport included a diffusion component, which reduced the amplitude and brought about the observed overlap of the lines [102].

4.3. An Analysis of the Material Parameters that Control the Charge Transport in Detectors

The aforementioned data on detection of alpha particles are used with good results in analyzing the most important parameters of SiC as a medium for detection of hard radiation. These parameters include the mean energy for formation of an electron–hole pair ε, the diffusion length for holes $L_D = (D\tau_0)^{1/2}$, the degree of inhomogeneity of the hole lifetime $\Delta\tau/\tau_0$ in the diode-structure base, and the lifetime of charge carriers until they become localized at the capture centers during the drift

in the SCR. Here, D is the diffusion coefficient and τ_0 is the mean lifetime of holes in the base.

4.3.1. Determination of the mean energy for formation of an electron–hole pair. The energy dissipated in the film E is determined first in order to calculate ε using mathematical simulation of the slowing-down of an alpha particle (the TRIM software package [103]). As mentioned above, the detected signal is proportional to the charge generated by a particle $Q_0 = eN$ (N is the number of produced electron–hole pairs and e is the elementary charge). This circumstance makes it possible to write the relation $N = E/\varepsilon = E_{sat}/\varepsilon_{Si}$. Here, $\varepsilon_{Si} = 3.62$ eV is the energy required for generation of an electron–hole pair in Si and E_{sat} is the experimental saturation energy (see Fig. 6); the value of E_{sat} is determined from the signal calibration using a silicon detector. Thus, we use the data shown in Fig. 6 to find that $\varepsilon = 8.6$ eV, which is close to the value $\varepsilon = 8.4$ eV reported by Rogalla *et al.* [104].

4.3.2. Determination of the hole diffusion length. Diffusion–drift transport was previously considered [105, 106] for the case of the steady-state and spatially uniform generation of charge carriers. As a result, the following expression, which is equivalent to that for the case of pulsed ionization in detectors, was derived:

$$Q/Q_0 = 1 - \lambda = (W + L_D)/d. \quad (3)$$

Here, $\lambda = 1 - Q/Q_0$ accounts for the deficit in the detected charge Q.

In the case of generation of charge carriers by alpha particles in thin films ($R > d$), dE_α/dx is assumed to be a linear function of x. This assumption complicates formula (3) but makes it possible to carry out the fitting procedure for the function $\lambda(W)$ using two parameters, L_D and d (Fig. 8) [99]. The quantity λ was calculated using the data in Fig. 6 as $\lambda = (E_{sat} - E)/E_{sat}$, and the value of W was determined from the capacitance measurements. As a result, we determined the quantity L_D ($L_D = 2.42$ μm) and refined the value of d ($d = 9.76$ μm).

4.3.3. The shape of the pulse-height spectrum and its relation to the lifetime of holes τ. The statistics of the signal amplitude manifests itself in the shape of the spectral line and is a specific characteristic of detectors. It is common practice to describe the straggling in the signals using the full width at the half-maximum (FWHM) of the line. The origin of the straggling is related to a number of factors; however, nonequilibrium-carrier transport is the dominant mechanism of straggling if the charge transport is incomplete. The shape of the line was analyzed previously [99, 107] taking into account special features of the charge-carrier diffusion characteristic of SiC.

The question of the shape of the line is also important methodologically since the use of alpha particles makes it possible to assess the microscale nonuniformity of τ over the film area [107]. Indeed, the tracks of alpha particles contain dense clusters of electron–hole pairs and have a diameter of ~10 μm (taking into account the spread caused by the diffusion and drift). Therefore, the magnitude of charge generated by each particle depends on the conditions of the carrier transport in a microscopic volume. The statistics of distribution of lifetime τ over the sample surface manifests itself as a result of random incidence of particles upon the detector. It is important that the charge-carrier lifetime is the parameter that is most sensitive to structural defects.

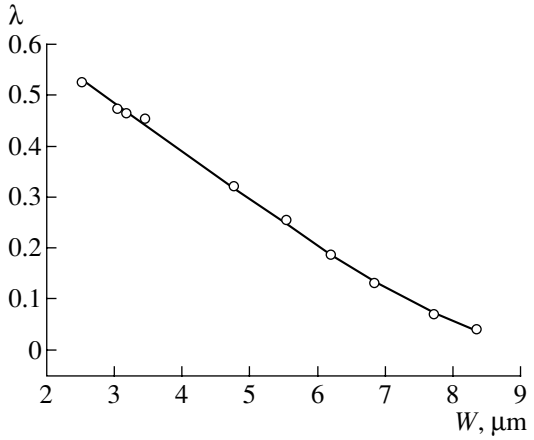

Fig. 8. Dependence of the signal deficit on the position of the SCR boundary. Circles correspond to the experimental data, and the solid line represents the result of the approximation according to Lebedev *et al.* [99].

We now consider the calculation of the spectrum shape. The pulse-height spectrum is plotted as $dN/dq = f(q)$, where dN is the number of pulses within the pulse-height range dq and $q = Q/Q_0$. In order to plot the spectrum, Strokan [107] used the identity $dN/dq = (dN/d\tau) \cdot (d\tau/dq)$; thus, the problem amounted to determining the shape of distribution for τ and the form of the function $q = f(\tau)$. The distribution of $dN/d\tau$ was assumed to be Gaussian with variance σ since a Gaussian function is most probable under conditions of small deviation of the parameter τ from the mean value τ_0, i.e., $|\tau - \tau_0| < \tau_0$. The FWHM of the spectrum as $\Delta\tau = 2.35\sigma$ was introduced similarly to the pulse-height spectrum. For simplicity, the charge-carrier generation rate was assumed to uniform over the film depth; the form of $d\tau/dq$ was then determined from expression (3). As a result, the following system of equations was derived (with numerical factors discarded):

$$dN/dq = (\tau/\tau_0)^{1/2}\exp[-(\tau/\tau_0 - 1)^2/0.362(\Delta\tau/\tau_0)^2],$$
$$q = (W + L_D\sqrt{\tau/\tau_0})/d. \quad (4)$$

Three dimensionless parameters in Eqs. (4), i.e., W/d, L_D/d, and $\Delta\tau/\tau_0$, affect the shape of the pulse-height spectrum in different ways. For example, the quantity W/d only shifts the position of the peak without affecting the value of FWHM. In contrast, the nonuniformity of τ only affects the FWHM of the spectral

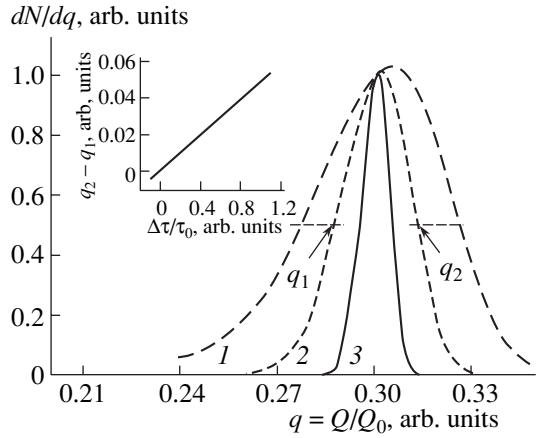

Fig. 9. Calculated shape of the pulse-height spectrum for various degrees of nonuniformity of lifetime of holes that diffuse in the base (see [99]). $\Delta\tau/\tau_0$ = (*1*) 100, (*2*) 50, and (*3*) 20%. $W/d = 0.2$ and $L_D/d = 0.1$. The width of the spectral line as a function of $\Delta\tau/\tau_0$ is shown in the inset.

line. Finally, the values of L_D/d affect the spectrum as a whole.

The plotting of the spectrum for several values of $\Delta\tau/\tau_0$ showed that the spectra were symmetric up to a nonuniformity of 50% ($\Delta\tau/\tau_0 = 0.5$) [99]. As the value of $\Delta\tau/\tau_0$ increases to unity, an asymmetry arises owing to the appearance of an extended region of small amplitudes at the left-hand wing of the spectrum. However, the value of FWHM is a linear function of $\Delta\tau/\tau_0$ in the entire range of $\Delta\tau/\tau_0$ under consideration (see inset in Fig. 9).

Moreover, the dependence FWHM = $f(L_D/d)$ was also found to be linear with a slope that was proportional to $\Delta\tau/\tau_0$. As a result, the quantity FWHM is defined as

$$\text{FWHM} = 0.48(\Delta\tau/\tau_0)(L_D/d). \qquad (5)$$

It can be seen that the line width is independent of the value of W/d, i.e., the bias voltage. The latter circumstance corresponds to the formulation of the problem where fluctuations in the detected charge are related to the stage of the charge-carrier diffusion and to the results of the measurements mentioned in 4.2.

The shape of the pulse-height spectrum was recorded for films with $L_D = 2.4$ μm and $d = 9.76$ μm; as a result, the value FWHM = 0.075 was obtained. According to formula (5), this value corresponds to $\Delta\tau/\tau_0 = (0.075/0.48)(d/L_D) \approx 0.6$, which almost coincides with the degree of nonuniformity determined in studying the charge-carrier transport in detector-grade silicon.

4.3.4. The drift transport and the capture time of charge carriers. We first consider the calculated parameters. The problem concerning the drift of charge carriers in a linearly varying field was considered by Eremin *et al.* [108]. In the case of "thin" SiC detectors, one should additionally take into account the fact that the charge-carrier generation rate increases linearly with the coordinate, and one should determine the mean charge magnitude detected experimentally under specified conditions.

The concentration of charge carriers as a function of the coordinate x in the course of their generation at a point y was determined first as a result of calculations. The charge $q(y)$ induced at the electrodes was then determined, and finally the mean value of this charge was calculated taking into account the generation-rate profile $G(y)$. For example, the above procedure yields the following formulas for holes:

$$p(x) = G(y)\exp\left(-\int_y^x \frac{dx}{\mu_h\tau_h F}\right),$$
$$q(y) = \frac{1}{d}\int_y^d p(x)dx, \qquad (6)$$
$$\bar{q} = \frac{1}{d}\int_0^d G(y)q(y)dy.$$

Here, F is the electric-field strength, μ_h is the hole mobility, and τ_h is the lifetime of holes until they are localized at the capture centers. The charge q is normalized to the value determined by the absorbed energy.

For simplicity, the capture rate is assumed to be low and is given by the linear term in the expansion of the exponential function. For a uniform field ($F(x)$ = const) and equiprobable generation rate ($G(y) = 1$), the solutions are descriptive in form and are the same for both electrons and holes. In the notation for holes, we have

$$q(y) = (1 - y/d)\left[1 - \frac{d-y}{2\mu_h\tau_h F}\right],$$
$$\bar{q} = 0.5\left(1 - \frac{d}{3\mu_h\tau_h F}\right). \qquad (7)$$

The linear behavior of $F(x)$ complicates relations (7) by introducing a logarithmic dependence on voltage [108]. It is worth noting that the identity of expressions for the charges transported by electrons and holes is retained in the case of a uniform generation rate of charge carriers. The charge-carrier generation rate that is nonuniform over the depth gives rise to different formulas for electrons and holes. The expressions become less clearly conceived. However, although these expression are cumbersome, they make it possible to determine τ_h using this parameter as an adjustable parameter [99].

We now consider the experimental data. The charge losses under the drift conditions can be analyzed using the data shown in Fig. 6. The voltage dependence of losses should be compared with calculated dependences on the value of τ_h. The small value of rms deviation serves as the criterion for agreement between

Table 6. Energy levels, concentrations, and impurities involved in a defect for trapping centers detected in SiC with the use of DLTS and ICTS [109]

Defect type	*S*0	*S*1	*S*2	*S*3	*S*4	*S*5
Energy, eV	0.10	0.19	0.32	0.91	0.40*	0.75*
Concentration, cm^{-3}	2×10^{11}	8.9×10^{12}	6×10^{11}	2.2×10^{13}	4.5×10^{12}	1.4×10^{13}
Impurity	Nitrogen	Chromium		Vanadium		

* At the interface between Au and epitaxial SiC film.

experimental and calculated values. The rms deviation was found to be much smaller in the case of the predominance of losses in the hole charges. The value obtained for the hole lifetime is equal to 35 ns. This value is smaller than that determined from the diffusion transport (62 ns; see Fig. 8, where L_D = 2.42 μm was found). This difference may be related to dissimilar occupation of the capture centers: diffusion occurs under conditions of equilibrium occupation of centers, whereas drift proceeds in nonequilibrium conditions where the occupancy of the centers under consideration is much lower.

The aforementioned results illustrate the methodological potential that follows from analyzing diffusion–drift transport of a nonequilibrium charge in diode structures of detectors. In this context, the question of how analytical expressions for describing the charge deficit and the shape of the amplitude spectrum are derived on the basis of known assumptions was assessed. These expressions are used to determine the key parameters of the charge-carrier transport: the lifetimes of charge carriers in the course of their drift, the diffusion length of nonequilibrium charge carriers in the base, and the degree of lifetime nonuniformity over the film area.

Nava *et al.* [109] used the DESSIS software package [110] to describe the diffusion–drift transport of charge carriers. Films of a higher structural quality were used, and unprecedentedly high values of charge-carrier lifetimes (500 ns and 95 μs for holes and electrons, respectively) were obtained.

The origin of the centers that capture the charge carriers was studied by Nava *et al.* [109] using DLTS and isothermal capacitance transient spectroscopy (ICTS). Comparison of the results obtained by the above methods made it possible to determine the characteristics of traps with a high accuracy, including the shallow-level traps that are not resolved by DLTS at the specified temperatures. The data on the energy position of the capture states, their concentration, and their possible relation to impurities are summarized in Table 6.

Thus, we may state that the level of drift-transport parameters that ensures almost 100% efficiency of charge transport is undoubtedly attained in modern SiC films. How to further decrease the impurity concentration, which would make it possible to attain larger widths of SCR, is a problem that remains to be solved.

Recent results of studies in this field seem to be very encouraging. For example, Kimoto *et al.* [111] attained a reproducible difference concentration of impurities of $(1–3) \times 10^{13}$ cm^{-3}. It is planned that the total concentration of traps will be reduced to 5×10^{11} cm^{-3}. The resulting SiC material approaches silicon in purity and makes it possible to fabricate detectors that are designed to operate with short-range ions and have a completely depleted base with a thickness of ~100 μm.

Good results were also obtained with respect to the formation of blocking contacts (shallow p^+–n junctions) in the detectors. The contact problem is solved by using an Al implantation [112, 113]. As a result, SiC structures reliably detect alpha particles at temperatures as high as 500°C.

4.4. The Use of SiC-based Detectors for Detection of Penetrating Radiation

4.4.1. Spectrometry of X-ray radiation. In order to ensure the mode of spectrometry, it is necessary that a complete deposition of the particle (photon) energy occurs in the detector's operation volume. In this context, the data reported by Bertuccio *et al.* [114, 115] and concerned with X-ray radiation spectroscopy with an energy $E_\gamma < 60$ keV are of interest. In this energy region, the mechanism of photoabsorption with transfer of the photon energy to the generated photoelectron is dominant. The photoelectron ranges increase superlinearly with the energy ($\propto E_\beta^{1.4}$); nevertheless, these ranges do not exceed 10 μm. Therefore, the photoelectron energy (especially, for E_γ < 20 keV) will be completely absorbed in the SCR of the detector, which is exactly characteristic of the spectrometry mode.

Bertuccio and Casigaghi [115] used *n*-4*H*-SiC films produced by CREE Research Inc. [116]. The films were 70-μm thick and had a difference impurity concentration of 9×10^{14} cm^{-3}. Special technology was used to form a Schottky barrier with an area of 0.03 mm^2 on an epitaxial layer. Spectrometric measurements were carried out at the reverse voltage of 300 V. The choice of this voltage was the result of compromise between the desire to attain an extended SCR (W = 18 μm) and the requirement for a moderate noise power. The average electric-field strength in these conditions exceeded 10^5 V/cm. However, the reverse-current density was no higher than 5×10^{-12} A/cm^2. For comparison, the

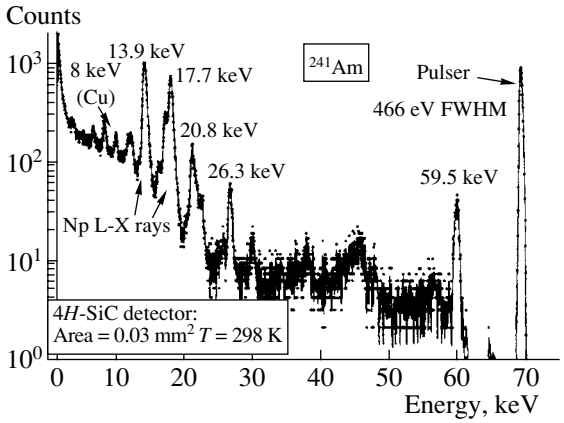

Fig. 10. Spectrum of ^{241}Am X-ray radiation measured at room temperature using a SiC detector (see [115]). The noise-induced straggling of the line was generated by a stable-amplitude oscillator (FWHM = 466 eV).

reverse-current densities in advanced silicon detectors are in the range $(0.5–1.0) \times 10^{-9}$ A/cm^2.

In Fig. 10, we show the ^{241}Am X-ray spectrum detected at 25°C; it can be seen that the characteristic X-ray energies are well resolved. The linearity of detected signal is retained in the entire range of measured peak energies (8.0–59.5 keV). However, it should be taken into consideration that the measured intensities of the lines are appreciably decreased as the energy of X-ray photons increases. This fact is related to a drastic decrease in the absorption of high-energy photons in the SCR due to the small width of this region.

An increase in the SCR width would reduce both the decrease in the line intensity and the detector capacitance (at the unchanged detector area). A decrease in the capacitance would make it possible to reduce the noise power.

4.4.2. Dosimetry of electrons and gamma-ray photons. The response of SiC detectors to the above types of ionizing radiation is of interest from the standpoint of radiotherapy. The detectors were typically irradiated with 22-MeV electrons and 6-MeV photons; the latter were produced by electrons accelerated to an energy of 6 MeV in a linear accelerator. The range of absorbed doses was 1–10 Gy at intensities of 2–7 Gy/min [117].

In the above conditions of irradiation, the performance of dosimeters based on SiC, Si, and CVD diamond films was compared. It was found that the sensitivity of silicon dosimeters degraded and dropped to 35% after exposure to an electron dose of 3 kGy. The diamond films have a polycrystalline structure and exhibit an appreciable nonuniformity of properties. This nonuniformity significantly lowers the spatial resolution of the detector. In addition, so-called "pumping" is required to stabilize the detector's sensitivity. This pumping consists in preliminary exposure of the sample to the radiation of an X-ray tube (with an anode voltage of 50 kV) with a typical dose of 10 Gy [118].

The best results for electron dosimetry were obtained using Schottky diodes fabricated on epitaxial 4*H*-SiC films that had $N_d^+ - N_a^- = 2.2 \times 10^{15}$ cm^{-3}, were 30-μm thick, and were produced by CREE. The diodes operated at a bias voltage of 150 V. The dependence of the induced charge on the absorbed electron dose was linear in the range 1–10 Gy and had a slope of 16.37 nC/Gy.

In turn, in the case of irradiation with 6-MeV gamma-ray photons (with a dose rate of 2.1–6.5 Gy/min), the induced-current dependence on the dose was also linear and had a slope of 3.5×10^{-10} A min/Gy. The width of the active zone was $W + L_D = (8.5 + 12.2)$ μm.

However, an attempt to use a semi-insulating "bulk" (230-μm thick) 6*H*-SiC sample failed: the sensitivity to electrons was too low. This fact should be related to the large number of structural defects. Recombination centers reduce the efficiency of charge transport, and microvoids bring about an increase in the dark currents.

The data listed in Table 7 make it possible to compare the performance of dosimeters of various types; it can be seen that diode structures based on epitaxial SiC films are quite suitable for dosimetry of electrons and gamma-ray photons.

4.4.3. Detection of relativistic particles. Naturally, silicon carbide was among the materials considered as suitable when experiments with high radiation rates were planned at next-generation accelerators (such as the Large Hadron Collider at CERN).

The potential of SiC as a material for a track detector was studied by Rogalla *et al.* [119]. They used

Table 7. Comparison of sensitivity and the ratio of sensitivity to volume for a dosimeter based on epitaxial SiC, those for commercial (Scanditronix) Si-based dosimeters, and those for two dosimeters based on CVD diamond films [117]

Dosimeter	Voltage, V	Active volume, mm^3	Sensitivity, nC/Gy	Sensitivity/volume, nC/(Gy mm^3)
Silicon	0	0.295	150	509
CVD diamond	50	3.7	690	190
CVD diamond	400	4.7	420	90
Silicon carbide	150	0.06	16.4	273

Note: The silicon dosimeter had been preliminarily irradiated with 20-MeV electrons at a dose of 10 kGy so that the subsequent irradiation did not affect the sensitivity.

310-μm-thick semi-insulating 4*H*-SiC substrates produced by CREE. The contacts formed on both surfaces of the sample were ohmic. In addition, a guard ring was used, which made it possible to observe a linear current–voltage characteristic with a resistivity of 5.1×10^{10} Ω cm in the voltage range ±500 V.

In order to imitate high-energy particles, the ^{90}Sr electrons with the highest energy (2.2 MeV) were used. The signals produced by only the high-energy electrons that traveled through the sample and induced the lowest ionization in SiC were analyzed. In order to select these ionization events, a conventional silicon detector was installed behind the SiC sample. Signals from this detector that corresponded to an energy of ≤1 MeV were distinguished, whereas the signals corresponding to the absorption of an energy of >1 MeV were fed to the coincidence circuit. The tracks of the latter electrons In SiC contained 17000 electron–hole pairs.

Experiments showed that the signal and noise spectra were well resolved; however, two adverse factors were observed [119]. First, the carrier-transport efficiency was as low as $\eta \approx 12\%$. Second, the signal amplitude decayed exponentially with time constant $\theta = 14.2$ min. The above observations indicate that the value of the charge-carrier lifetime is small and deep levels are involved in the formation of the electric field. It is significant that the introduction of radiation defects (as a result of irradiation with 8-GeV protons at a dose of 4.16×10^{14} cm^{-2}) brought about an additional decrease in η by 23% and in θ to 3.6 min. Simultaneously, the resistivity of the samples increased threefold.

We emphasize that Rogalla *et al.* [119] were the first to design a detector based on semi-insulating 4*H*-SiC. The observed signal instability and the relatively low efficiency of the charge transport should be attributable to the inadequate quality of the material (corresponding approximately to the state of the art in 1998). It will be recalled that the low sensitivity of semi-insulating SiC to electrons was also observed by Bruzzi *et al.* [117].

4.4.4. Detection of neutrons in the reactor channel. The problem of detection is related to the determination of neutron fluxes and the control of the reactor operation. It is characteristic that the solution to this problem is based simultaneously on the high radiation, thermal, and chemical stability of SiC.

Since neutrons do not directly produce ionization, the reactions in which the neutron energy is transferred to other (short-range) ionizing particles, such as alpha particles or fission fragments that can be detected by SiC diodes, should be used. As far back as the 1960s, good agreement between the data for SiC diodes coated with a ^{235}U layer and the results of measurements using the conventional method of activation of gold foils was observed [120].

It was also ascertained that SiC-based diodes can detect alpha particles after having been irradiated with high doses of thermal neutrons (6×10^{15} cm^{-2}). Regarding fast neutrons (with energies higher than 1 MeV), the dose can be as high as ~10^{17} cm^{-2} [121]. SiC-based detectors exhibited a radiation resistance which exceeded that of silicon detectors by almost a factor of 5 when the ^{233}U fission fragments were detected directly in the reactor channel [98]. The neutron-flux density was 10^8 cm^{-2} s^{-1}, and the exposure time was 340 h. In this context, the feasibility of evaluating a neutron spectrum if SiC detectors are complemented with a set of ^{233}U, ^{234}U, ^{235}U, ^{238}U, ^{232}Th, and ^{239}Pu converters was discussed.

Recent progress in the field of the growth of high-purity SiC films makes it possible to solve a problem that is typical of reactors and consists in measuring the field of combined neutron and gamma-ray radiation. The experiments were carried out in the TRIGA reactor [122, 123] under conditions of low-power radiation (50–290 W). An array of 22 Schottky diodes with diameters of 200 or 400 μm was used. The diodes could be connected in parallel, thus increasing the total area. A LiF layer installed near the detector surface served as a converter; the neutron flux was measured on the basis of triton counts, according to the reaction ^{6}Li(n, α)^{3}H.

The portions related to direct detection of the background of tritons and gamma-ray photons are resolved in the observed pulse-height spectrum. As a result, these radiation types are detected separately; consequently, it was possible to determine the distributions of neutrons and gamma-ray photons in the form of a function of the distance from the channel's center line. The measurements take about 30 min when 12 diodes are connected in parallel.

In determining gamma-ray and neutron fluxes, the SiC detectors showed a high accuracy (the errors were 0.6 and 1.9%, respectively). We may state that small-size SiC detectors can be used with good results to monitor the operation not only of the reactor assemblies but also of its active zones.

4.5. Radiation Resistance of Detectors

The radiation resistance of SiC with respect to nuclear radiation was discussed to some extent in each of the previous subsections. We now turn our attention to the aforementioned (4.4.3) case of relativistic particles in connection with planned large-scale experiments at the Large Hadron Collider at CERN. In these experiments, detectors are expected to operate continuously for ten years. Furthermore, the doses of irradiation with relativistic particles range from 2×10^{14} to 5×10^{15} cm^{-2}, depending on the distance from the site where the beams interact. Under these conditions, the use of advanced silicon detectors encounters serious difficulties even at doses as low as ~10^{14} cm^{-2} [124].

First, the dissipated power increases appreciably (the reverse currents and the voltages corresponding to depletion of the structure increase). Second, the efficiency of nonequilibrium-charge transport and, correspondingly, the signal amplitude are reduced. In this

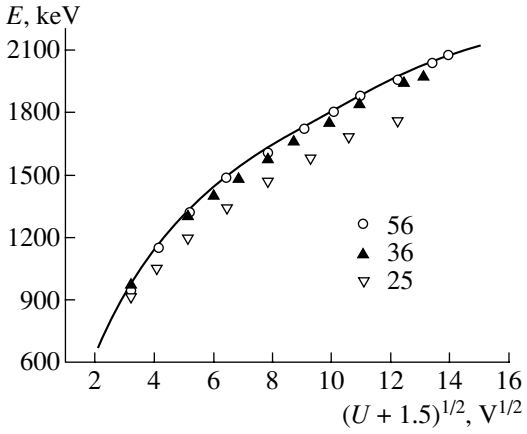

Fig. 11. Reverse-voltage dependence of the energy deposited by an alpha particle in the sensitive region of the detector's diode structure before irradiation with protons (see [126]). The numbers 56, 36, and 25 correspond to designations of the samples. The nonlinearity of the dependence (solid line) is caused by the nonuniform distribution of impurities in the SiC film.

context, Verbitskaya *et al.* [125] studied the results of cooling Si detectors and the feasibility of varying the field profile by controlled injection of charge carriers from the contact. Complication of the conditions of operation for silicon detectors has led to a search for materials with a higher radiation resistance.

Ivanov *et al.* [126, 127] analyzed the performance of a SiC detector irradiated with 1-GeV protons with a dose increasing from 3×10^{14} to 1.3×10^{15} cm^{-2}.

Schottky diodes that had a diameter of 600 μm and were formed by magnetron sputtering of Ni onto the surface of high-quality 6*H*-SiC films were used. The films were grown by sublimation epitaxy in vacuum [128]. The difference concentration of ionized impurities varied from 5×10^{14} cm^{-3} at the surface to 8×10^{15} cm^{-3} at depth $d = 7$ μm. Such a distribution of $N_d^+ - N_a^-$ concentration made it possible to form a pulling field in the diode structure, which increased the effective diffusion length of charge carriers [129].

The detectability of SiC structures was analyzed using ^{244}Cm alpha particles (see 4.2). The characteristics of the deep-level centers formed were determined using DLTS. A typical voltage dependence of the signal amplitude $E(U)$ is shown in Fig. 11. It is significant that the values of E for different samples almost coincide, which is indicative of the fairly high uniformity of SiC properties over the film area.

Irradiation with a dose of 3×10^{14} cm^{-2} reduced the value of L_D for holes by less than 30%; variations in $N_d^+ - N_a^-$ compared to initial values were insignificant.

Measurements of the spectrum of deep-level centers showed that only the concentration of *R* centers changed appreciably (see Table 8). Lebedev *et al.* [130] studied the introduction of these centers as a result of irradiation with 8-MeV protons; it was ascertained that these centers were related to vacancies. Therefore, the TRIM software package was used to compare the number of primary vacancies for proton energies of 8 MeV and 1 GeV. The ratio of these numbers was found to equal 110 : 1, which is a consequence of a decrease in the cross section for proton scattering by Si and C atoms as the proton energy increases.

Experimentally, concentrations of the *R* centers in the two above cases (irradiation with 8-MeV and 2-GeV protons) are related as 400 to 1. Thus, the result expected from the concept of primary defects is found to be inconsistent with the number of secondary (actual) centers that are formed in SiC as a result of physicochemical reactions. Evidently, there is a difference between the energy transferred to primarily displaced Si and C atoms in the course of defect production by the 8-MeV and 1-GeV protons.

In the case of irradiation with high-energy protons, more compact Frenkel pairs are formed; recombination of vacancies and interstitial atoms occurs more efficiently for these pairs. Accordingly, a lesser number of vacancies is transferred from the tracks of recoil atoms to the film bulk with subsequent formation of the *R* centers. Emtsev *et al.* [131] considered in detail the above mechanism of recombination for components of Frenkel pairs (using silicon as an example) taking into account the possible recharging of these components. We note that the opposite situation of a low recombination rate for vacancies and interstitial atoms, which is characteristic of diamond, raises the crucial question as to the radiation resistance of diamond [132].

Irradiation with a total proton dose of 1.3×10^{15} cm^{-2} [127] brought about certain changes in the characteristics of the structure. The conductivity of SiC became heavily compensated. In addition, a high-resistivity base was formed in the diode structure of the detector; the Maxwell relaxation time in this base exceeded the characteristic time of signal shaping by the instrumentation electronics. Under these conditions, a characteristic falloff of the signal by W/d times should be observed (the signal amplitude is proportional to $\propto W^2 \propto U$) if the structure is incompletely depleted [133]. However, it was ascertained for alpha particles that penetrated through the base that relaxation of the base in structures with semi-insulating SiC films is promoted as a result of the presence of a high concentra-

Table 8. Deep-level centers in SiC before and after irradiation with 1-GeV protons at a dose of 3×10^{14} cm^{-2} according to DLTS measurements [126]

Center type	Energy, eV	Concentration of the centers, cm^{-3}	
		before irradiation	after irradiation
E_1/E_2	0.35–0.4	$(1–2) \times 10^{13}$	$(1–2) \times 10^{13}$
R	1.1–1.2	$<5 \times 10^{12}$	5×10^{13}

tion of nonequilibrium charge carriers in the track [134, 135]. Indeed, the dependence $W_{\text{eff}} = f(U + 1.5)^{1/2}$ remained linear after irradiation with an alpha-particle dose of 1.3×10^{15} cm^{-2} [127]. However, the accuracy of experiment gave no way of separating the terms of the quantity $W_{\text{eff}} = W + L_D$.

Figure 12 illustrates the value of the charge transported in the structure for two proton doses. The voltage required for attaining the same value of the charge after the second dose was found to be higher by a factor of 3. Most likely, this fact may be related to the existence of local inhomogeneities in the course of compensation of the material. The same conclusion can be reached if we take into account that the WFHM of the spectrum is reduced to 10%; i.e., the conditions of charge-carrier transport through the detector bulk become leveled off.

The drift length of holes in an electric field F was determined [126] from the expression

$$L_F^h = (\mu_h \tau_h)F = (L_D)^2(Fe/kT), \quad (8)$$

where k is the Boltzmann constant. Introducing $L_D = 1$ μm and $F = 10^5$ V/cm (after the irradiation with a dose of 3×10^{14} cm^{-2}), we obtain $L_F^h = 400$ μm for the hole transport.

The drift length of electrons was only estimated. The estimation was based on the initial value of the product of the mobility by lifetime for electrons $\mu_e\tau_e = 7 \times 10^{-9}$ cm^2/V. This value was obtained [134] for SiC irradiated with 8-MeV protons at a dose of 8×10^{15} cm^{-2}. Assuming that the decrease in τ_e was caused by the R centers, a coefficient accounting for the number of produced R centers for 1-GeV protons with a dose of 3×10^{14} cm^{-2} was introduced. As a result, we obtain $L_F^e \leq 1$ cm. Thus, we may assume that the drift lengths of charge carriers are satisfactorily large for detectors with an SCR (operating zone) with a width of several hundreds of micrometers. Data on the drift length of charge carriers in the structures irradiated with a total proton dose of 1.3×10^{15} cm^{-2} were not reported [127].

It is significant [126, 130] that the proton energy only slightly affects the nature of the radiation defects produced. In both cases (the 8-MeV and 1-GeV protons), the main role is played by the R center with a level that is 1.1–1.2 eV below the bottom of the conduction band.

To summarize the results for SiC detectors, we may state that a proton dose of 3×10^{14} cm^{-2} represents [126, 127] a threshold for radiation-induced changes in the properties of SiC with a given level of purity. If the dose does not exceed the threshold value, the lifetime of charge carriers does not decrease appreciably and the conductivity is not compensated significantly as a result of irradiation.

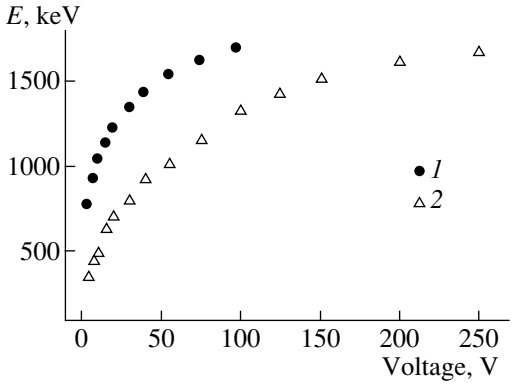

Fig. 12. Signal amplitude as a function of applied voltage for relativistic-proton doses equal to (*1*) 3×10^{14} and (*2*) 1.3×10^{15} cm^{-2}.

4.6. Feasibility of Signal Amplification

We specified above the quantities that are characteristic of charge-carrier transport in SiC. We also gave examples of the successful performance of SiC-based detectors in a number of important fields. It is evident that the main disadvantage of SiC detectors is the small width of the active (operating) zone. This circumstance is especially perceptible when penetrating (weakly ionizing) radiation is detected. In this context, it seems to be of interest to consider the feasibility of increasing the effective width of the operating zone, for example, by attaining a signal amplitude larger than the energy dissipated in the detector.

4.6.1. The principle of a through conducting channel. This principle was formulated in the late 1950s and was applied to semi-insulating films with monopolar conductivity [136, 137]. While the contacts block the transfer of charge carriers from the external circuit in detectors of the ionization-chamber type, the opposite situation (the contacts did not limit the current) was considered in [136, 137]. It was also a necessary condition that a highly ionizing particle penetrate through the film. Consequently, conducting tracks of particles shunted the film resistance.

If the monopolar character of conductivity is caused by the short lifetime of charge carriers (to be precise, holes), the nonequilibrium holes produced by a particle are localized at the capture centers and are immobilized. In contrast, the transport of electrons is possible through the track and external circuit. Thus, a through conducting channel comes into existence in the semi-insulating film. The charge Q transported through the circuit is related to the charge Q_0 generated by ionizing particles by the following expression:

$$Q = Q_0[(\mu_e\tau_e)_e F/d] = Q_0(\tau_e/t_{\text{dr}}). \quad (9)$$

Here, $t_{\text{dr}} = d/\mu_e(F)$ is the time of electron drift through the film. If the inequality $\tau_e/t_{\text{dr}} > 1$ is valid, amplification of the signal is observed.

A similar situation was simulated [134] for the p^+–n–n^+ structures that are based on 6*H*-SiC films with introduced radiation defects and biased in the conducting direction. The films had the initial concentration of uncompensated donors $N_d^+ - N_a^- = 4.5 \times 10^{16}$ cm^{-2} and a thickness of several micrometers. Irradiation with 8-MeV protons with a dose of 8×10^{15} cm^{-2} brought about an increase in the film resistivity to 5×10^9 Ω cm.

When alpha particles penetrated through the film, the bias dependence of the signal was linear in accordance with expression (9) and corresponded to $\mu_e\tau_e = 7 \times 10^{-9}$ cm^2/V. A gain of 1.7 was attained at a bias voltage of 25 V.

Strokan *et al.* [134] attribute the fact that the gain is low to the high total concentration of structural defects in the film (~10^{17} cm^{-3}). Therefore, the experiment described above clarifies to a great extent the principle of amplification but leaves the attainable gain unclear.

4.6.2. Amplification in a transistor structure. The charge amplification with the same coefficient τ_e/t_{dr} can also be attained in a transistor structure (see, for example, [138, 139]). The corresponding experiment with SiC films was described elsewhere [140, 141].

p-6*H*-SiC films served as starting base regions for the structures under consideration: films with a thickness of ~10 μm were grown by sublimation on n^+-type substrates. The difference concentration of impurities $N_a^- - N_d^+$ in the films was equal to 2.8×10^{15} cm^{-3}. A Schottky barrier obtained by sputtering Ni was used as the second electrode.

The structures were studied in the mode of connection with a floating base and were irradiated with 5.8-MeV ^{244}Cm alpha particles (the range in SiC was equal to 20 μm) directed onto the side of the Schottky barrier. The nonequilibrium charge produced in the base corresponded to the absorption of the energy that was no higher than 2 MeV. The shape of the signal spectrum and the dependence of the mean signal amplitude on the bias voltage *U* applied to the structure were measured using the conventional pulse-height analysis (see 4.2).

The barrier regions in the structures differed widely. The Schottky barrier corresponded to an abrupt junction; however, the change in the *p*-type conductivity was gradual on the side of the n^+-type substrate. Therefore, we compared two polarities of connection: the role of the collector was played either by the p–n^+ junction of the substrate (case I) or by the Schottky barrier (case II).

In case I, the signal amplitude *E* exceeded only twofold the value of energy deposited by a particle in the base. The dependence *E*(*U*) was sublinear and exhibited a tendency towards leveling off. Strokan *et al.* [141] attribute this behavior of the signal to the low injection efficiency of the emitter (the Schottky barrier) and short lifetime of charge carriers at the barrier. The shape of the spectral line was Gaussian (FWHM ≈ 10%), which indicates that the conditions of charge transport in the film were fairly uniform.

In case II, where the Schottky barrier acted as a collector, the dependence *E*(*U*) was superlinear. The signal amplitude now corresponded to 60–80 MeV. The shape of the spectrum was found to be Gaussian, as in case I; the straggling was FWHM ≈ 9%, nearly the same as in case I.

Strokan *et al.* described qualitatively the results reported in [141] in the context of the model suggested by S.M. Ryvkin in his monograph [138]. The primary minority charge carriers (in the case under consideration, electrons) generated in the base when an alpha particle is slowed down diffuse to the emitter and collector junctions where these carriers become involved in the drift caused by existing fields. Nonequilibrium holes are found residing in a potential well and charge it positively in reference to the emitter. Variation in the emitter–base potential difference increases the secondary-electron current injected by the emitter.

In order to describe the effect quantitatively, it was assumed that the primary-current gain in the phototransistor amounted to $(1 - \alpha_T)^{-1}$, where α_T is the transport coefficient for electrons in the base. Thus, it was implicitly assumed that the emitter efficiency was equal to unity. The expression for α_T in the case when transport of the charge enters into the base with a δ-shaped voltage pulse applied to the emitter–base junction is written as

$$\alpha_T = [(d - W)/L_D]/\sinh[(d - W)/L_D], \qquad (10)$$

where *W* and L_D are the SCR width at the collector junction and the diffusion length of electrons, respectively. Expression (10) forms the basis for a final formula used in [141] to describe the detector signal in relation to *d*, *W*, and L_D.

The dependence *E*(*U*) was measured in the course of the experiment. Therefore, the values of *U* were converted to the values of *W*. In Fig. 13, we show the results of fitting the calculated values of α and L_D to experimental data for two samples.

Alpha particles belong to the class of highly ionizing radiation. At the same time, the response of transistor structures to weakly ionizing radiation (X- and gamma-ray radiation, high-energy particles), in which case the initial dissipation of energy in the film is insignificant, is more important in practice.

Strokan *et al.* [102] detected the X-ray and optical photons. In the case of X-ray detection, the radiation of an X-ray tube was used (anode voltage, 20 kV). For optical-photon detection, the detectors were exposed to light from a mercury lamp. The transistor structures of detectors included a thin (~5 μm) base doped to the level of $N_a^- - N_d^+ = (1–3) \times 10^{-15}$ cm^{-3}. The area of the Schottky barriers was 1.2 mm^2.

The response to the X-ray radiation as a function of U was superlinear. In Fig. 14, we show a portion of the dependence of photocurrent on $(U + 1.5)^{1/2}$; the current was normalized to its value of 13.5 nA at $(U + 1.5)^{1/2} = 4.1\ V^{1/2}$. It is significant that a drastic increase in the current (by a factor of 25 relative to the initial value) is observed within a comparatively narrow range of variations in the argument.

When processing the data of Fig. 14, Strokan *et al.* [102] used the following formula for the steady-state collector current (see [143]):

$$I_c = I_{ph}/(1 - \alpha_T), \quad \alpha_T = \{\cosh[(d - W)/L_D]\}^{-1}. \quad (11)$$

Here, I_{ph} is the primary photoelectron current in the collector and α_T is the transport coefficient for electrons injected into the base owing to a steady-state photovoltage at the emitter–base junction. An expression for I_{ph} in [102] accounted for both the drift transport of electrons from the SCR with the width W and the contribution of electron diffusion from the neutral base.

The comparison shown in Fig. 14 between the experimental data and the results of calculations yielded film thickness $d = 4.66$ μm and diffusion length $L_D \approx 0.35$ μm, which was consistent with the film growth conditions.

A semitransparent Ni electrode was used when charge carriers were generated by optical phonons. Similar processing of dependences $I_c(U)$ yielded $d = 4.67$ μm, which coincided with the corresponding value obtained in the case of X-ray radiation. However, the quantity $L_D = 0.83$ μm exceeded by almost a factor of 2 the value of L_D obtained from the data in Fig. 14. This increase in L_D can be attributed to the fact that the currents in the case of optical excitation of charge carriers were larger by two orders of magnitude than those under excitation with X-ray photons.

It is significant that the signal amplification observed by Strokan *et al.* [102, 141] is not noticeably affected by the features of the charge-carrier generation. The polar cases here are the effects of alpha particles and X-ray photons. Individual alpha particles produce dense charge-carrier tracks in the shape of cylinders with a diameter of ~10 μm, whereas the X-ray photons generate charge carriers with a low density and equiprobably throughout the entire volume of the base in a transistor structure. However, the superlinear increase in the signal amplitude with almost identical amplification coefficients is observed in both cases. As a result, the features of radiation-induced introduction of nonequilibrium charge carriers into the base have almost no effect on the resulting signal. This inference is consistent with a phototransistor model according to which the current flowing through the base is controlled by photovoltage at the emitter–base junction; this photovoltage is generated by the primary charge itself.

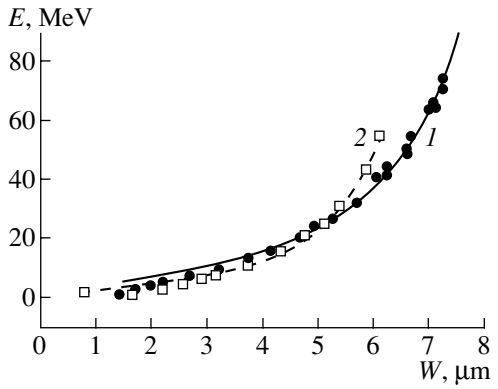

Fig. 13. Dependence of the alpha-particle signal expressed in energy units on the width of the space-charge region at the collector junction (Schottky barrier). The squares and filled circles correspond to experimental data, and the lines represent the results of approximation (see [140]) for the following values of adjustable parameters: diffusion length $L_D = 8.85$ and 5.85 μm and film thickness $d = 10.75$ and 8.53 μm for samples *1* and *2*, respectively.

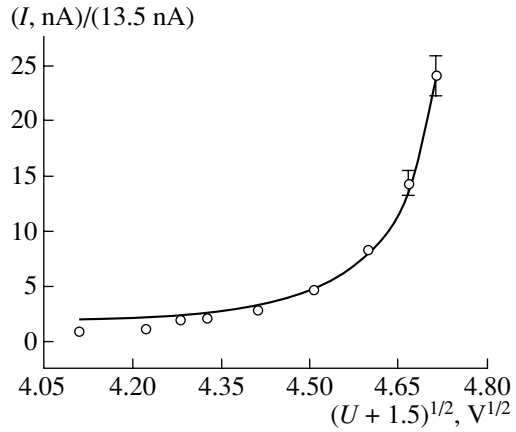

Fig. 14. Dependence of the current induced by the radiation of an X-ray tube on the voltage applied to the detector's diode structure. The solid curve represents the results of approximation (see [102]) at a current normalized to the value of 13.5 nA. The values of the parameters are the following: film thickness $d = 4.66$ μm and electron diffusion length $L_D = 0.35$ μm. The voltage applied to the anode of the X-ray tube was equal to 20 kV.

Thus, internal amplification of the signal by at least tenfold can be accomplished in detectors based on SiC films with a reduced concentration of impurities. This amplification is attained in structures that are comparatively easy to fabricate and include the Schottky barrier; the latter is used as the collector. It is important from the practical standpoint that comparatively thin (on the order of tens of micrometers in thickness) SiC films can be used to detect penetrating radiation. Significantly, the effective thickness of these films is found to be larger than the initial thickness by a factor that is equal to the signal amplification coefficient.

5. CONCLUSION

Naturally, recent advances in the development of growth technology for SiC films have also affected the application field of SiC. In particular, interest in the use of SiC in nuclear physics and in technical applications of SiC as a detecting medium has been renewed. We attempted to present the results of studying the problem of SiC applications in the context of two approaches. First, we tried to give existing examples of using the potential of SiC in typical problems in physics and technology. Second, we did our best to clarify the relation between the detector characteristics and the key parameters of the material. We also mentioned methods for solving the inverse problem, i.e., the problem of determining the electrical characteristics of SiC samples from parameters of detector structures based on these samples.

Concerning the properties of radiation defects in silicon carbide, it is shown that, at room temperature, the concentrations of intrinsic defects that already exist in the material increases irrespective of both the growth technology of the material and the type of incident particles.

The radiation defects produced can be either donors or acceptors. In relation to 6*H*-SiC, this fact brings about, on the one hand, compensation of the material at room temperature and, on the other hand, an increase in $N_d^+ - N_a^-$ at temperatures higher than 600 K. In the case of 4*H*-SiC, the concentration of the acceptors introduced is prevalent. As a result, the concentration $N_d^+ - N_a^-$ is found to be lower than the initial concentration even at elevated temperatures. As a consequence, the estimation of the SiC radiation resistance cannot be restricted to measurements at room temperature because of the significant temperature dependence of the carrier-removal rate.

Numerical values of the radiation-defect production rate at least do not exceed the characteristic values for silicon, which is the main material in contemporary electronics.

Concluding our consideration of problems in SiC detectors, we note that recent progress attained in the growth technology of impurity-free and structurally perfect SiC films (with a density of micropipe defects of ~1 cm^{-2}) has transferred SiC to the class of materials suitable for producing detectors. At present, it is premature to state that an experimental batch of such devices has been fabricated. Publications dealing with research into the structures or testing of detectors in various operational conditions far outnumber those concerned with a direct solution to scientific and technical problems of nuclear physics.

However, the potential of SiC for fabricating a number of SiC-based customized detectors that retain their operation characteristics at high radiation loads, in conditions of an aggressive medium, and at elevated temperatures (as high as 500°C), has been clearly recognized. These specialized detectors can be used in systems for monitoring in acid-containing media with alpha-particle radioactivity and in systems that are designed for determining the fields of X- and gamma-ray radiation and retain normal operation after doses at least as high as tens of megarads. Other applications include SiC detectors for measuring thermal-neutron fields (with ^{10}B as the conversion medium), for detection of high-energy neutrons using the reaction $^{12}C(n_0, \alpha)^9Be$, and for analysis of narrow high-power pulses of X-ray radiation.

A separate class of problems comprises applications in medicine, which are related to the similarity of the stopping powers of silicon carbide and tissues of biological species (tissue equivalence).

ACKNOWLEDGMENTS

We thank Professor V.V. Kozlovskiĭ for his helpful discussion of the manuscript.

REFERENCES

1. *Problems in Radiation Technology of Semiconductors*, Ed. by L. S. Smirnov (Nauka, Novosibirsk, 1980).
2. *Physical Processes in Exposed Semiconductors*, Ed. by L. S. Smirnov (Nauka, Novosibirsk, 1977).
3. J. W. Corbett and J. C. Bourgoin, in *Point Defect in Solids* (Plenum, New York, 1975), Vol. 2, p. 1.
4. B. Hudson and B. E. Sheldon, J. Microsc. **97**, 113 (1973).
5. I. A. Honstvet, R. E. Smallman, and P. M. Marquis, Philos. Mag. A **41**, 201 (1980).
6. H. Inui, H. Mori, and H. Fujita, Philos. Mag. B **61**, 107 (1990).
7. W. Jiang, S. Theunthasan, W. J. Weber, and R. Grotzschel, Nucl. Instrum. Methods Phys. Res. B **161–163**, 501 (2000).
8. I. Lazanu and S. Lazanu, Preprint (Elsevier, 2002).
9. V. S. Balandovich and G. N. Violina, Cryst. Lattice Defects Amorphous Mater. **13**, 189 (1987).
10. A. A. Lebedev, Fiz. Tekh. Poluprovodn. (St. Petersburg) **33**, 129 (1999) [Semiconductors **33**, 107 (1999)].
11. H. Zhang, G. Pensl, P. Glasow, and S. Leibenzeder, in *Extended Abstracts of Electrochemical Society Meeting* (1989), p. 714.
12. J. P. Doyle, M. O. Adoelfotoh, B. G. Svensson, *et al.*, Diamond Relat. Mater. **6**, 1388 (1997).
13. C. Hemmingson, N. T. Son, O. Kordina, *et al.*, Mater. Sci. Eng. B **46**, 336 (1997).
14. C. Hemmingson, N. T. Son, O. Kordina, *et al.*, J. Appl. Phys. **81**, 6155 (1997).
15. T. Dalibor, G. Pensl, H. Matsunami, *et al.*, Phys. Status Solidi A **162**, 199 (1997).
16. M. Gong, S. Fung, C. D. Beiling, and Zhipu You, J. Appl. Phys. **85**, 7604 (1999).
17. V. S. Ballandovich, Fiz. Tekh. Poluprovodn. (St. Petersburg) **33**, 1314 (1999) [Semiconductors **33**, 1188 (1999)].

18. I. Pintilie, L. Pintilie, K. Irmscher, and B. Thomas, Appl. Phys. Lett. **81**, 4841 (2002).
19. M. Gong, S. Fung, C. D. Beiling, and Zhipu You, J. Appl. Phys. **85**, 7120 (1999).
20. H. J. von Bardeleben, J. L. Cantin, L. Henry, and M. F. Barthe, Phys. Rev. B **62**, 10841 (2000).
21. N. T. Son, B. Magnusson, and E. Janzen, Appl. Phys. Lett. **81**, 3945 (2002).
22. V. V. Evstropov and A. M. Strel'chuk, Fiz. Tekh. Poluprovodn. (St. Petersburg) **30**, 92 (1996) [Semiconductors **30**, 52 (1996)].
23. I. M. Pavlov, M. I. Iglitsyn, M. G. Kosagonov, and V. N. Solomatin, Fiz. Tekh. Poluprovodn. (Leningrad) **9**, 1279 (1975) [Sov. Phys. Semicond. **9**, 845 (1975)].
24. A. I. Veĭnger, A. A. Lepneva, G. A. Lomakina, *et al.*, Fiz. Tekh. Poluprovodn. (Leningrad) **18**, 2014 (1984) [Sov. Phys. Semicond. **18**, 1256 (1984)].
25. R. N. Kyutt, A. A. Lepneva, G. A. Lomakina, *et al.*, Fiz. Tverd. Tela (Leningrad) **30**, 1500 (1988) [Sov. Phys. Solid State **30**, 1500 (1988)].
26. A. I. Girka, V. A. Kuleshin, A. D. Mokroshin, *et al.*, Fiz. Tekh. Poluprovodn. (Leningrad) **23**, 1270 (1989) [Sov. Phys. Semicond. **23**, 790 (1989)].
27. R. N. Kyutt, A. A. Lepneva, G. A. Lomakina, *et al.*, Fiz. Tverd. Tela (Leningrad) **30**, 2606 (1988) [Sov. Phys. Solid State **30**, 1500 (1988)].
28. V. V. Evstropov, A. M. Strel'chuk, A. L. Syrkin, and V. E. Chelnokov, Inst. Phys. Conf. Ser. **137**, 589 (1994).
29. O. Okada, T. Kimura, T. Nakata, *et al.*, Inst. Phys. Conf. Ser. **142**, 469 (1996).
30. H. Matsunami and T. Kimoto, Mater. Sci. Eng. R **20**, 125 (1997).
31. V. Nagesh, J. W. Farmer, R. F. Davis, and H. S. Kong, Appl. Phys. Lett. **50**, 1138 (1987).
32. S. Kanazawa, M. Okada, J. Ishil, *et al.*, Mater. Sci. Forum **389–393**, 517 (2002).
33. G. C. Rubicki, J. Appl. Phys. **78**, 2996 (1995).
34. I. V. Il'in, E. N. Mokhov, and P. G. Baranov, Fiz. Tverd. Tela (St. Petersburg) **35**, 1409 (2001) [Phys. Solid State **35**, 1347 (2001)].
35. A. A. Lebedev, D. V. Davydov, A. M. Strel'chuk, *et al.*, Mater. Sci. Forum **338–342**, 973 (2000).
36. A. M. Strel'chuk, V. V. Kozlovskii, N. S. Savkina, *et al.*, Mater. Sci. Eng. **61–62**, 441 (1999).
37. A. A. Lebedev, A. M. Strel'chuk, V. V. Kozlovskii, *et al.*, Mater. Sci. Eng. **61–62**, 450 (1999).
38. A. A. Lebedev, A. I. Veĭnger, D. V. Davydov, *et al.*, Fiz. Tekh. Poluprovodn. (St. Petersburg) **34**, 1058 (2000) [Semiconductors **34**, 1016 (2000)].
39. A. A. Lebedev, A. I. Veinger, D. V. Davydov, *et al.*, J. Appl. Phys. **88**, 6265 (2000).
40. M. M. Anikin, A. N. Andreev, A. A. Lebedev, *et al.*, Fiz. Tekh. Poluprovodn. (Leningrad) **25**, 328 (1991) [Sov. Phys. Semicond. **25**, 198 (1991)].
41. A. Kawasuso, F. Redmann, R. Krause-Rehberg, *et al.*, J. Appl. Phys. **90**, 3377 (2001).
42. A. Kawasuso, F. Redmann, R. Krause-Rehberg, *et al.*, Mater. Sci. Forum **353–356**, 537 (2001).
43. M. F. Barthe, P. Desgardin, L. Henry, *et al.*, Mater. Sci. Forum **389–393**, 493 (2002).
44. A. A. Lebedev, D. V. Davydov, N. S. Savkina, *et al.*, Fiz. Tekh. Poluprovodn. (St. Petersburg) **34**, 1183 (2000) [Semiconductors **34**, 1133 (2000)].
45. A. Kawasuso, F. Redmann, R. Krause-Rehberg, *et al.*, Appl. Phys. Lett. **79**, 3950 (2001).
46. W. C. Mitchel, R. Perrin, J. Goldstein, *et al.*, J. Appl. Phys. **86**, 5040 (1999).
47. A. I. Veĭnger, V. A. Il'in, Yu. M. Tairov, and V. F. Tsvetkov, Fiz. Tekh. Poluprovodn. (Leningrad) **15**, 1557 (1981) [Sov. Phys. Semicond. **15**, 902 (1981)].
48. D. T. Britton, M. F. Barthe, C. Corbel, *et al.*, Appl. Phys. Lett. **78**, 1234 (2001).
49. H. J. von Bardeleben, J. L. Cantin, I. Vickridge, and G. Battisting, Phys. Rev. B **62**, 10126 (2000).
50. D. V. Davydov, A. A. Lebedev, V. V. Kozlovskii, *et al.*, Physica B (Amsterdam) **308–310**, 641 (2001).
51. V. V. Makarov and N. N. Petrov, Fiz. Tverd. Tela (Leningrad) **8**, 1602 (1966) [Sov. Phys. Solid State **8**, 1272 (1966)].
52. V. Makarov, Fiz. Tverd. Tela (Leningrad) **9**, 596 (1967) [Sov. Phys. Solid State **9**, 457 (1967)].
53. N. V. Kodrau and V. V. Makarov, Fiz. Tekh. Poluprovodn. (Leningrad) **15**, 1408 (1981) [Sov. Phys. Semicond. **15**, 813 (1981)].
54. L. Patrick and W. J. Choyke, Phys. Rev. B **5**, 3253 (1972).
55. V. V. Makarov and N. N. Petrov, Fiz. Tverd. Tela (Leningrad) **8**, 3393 (1966) [Sov. Phys. Solid State **8**, 2714 (1966)].
56. V. V. Makarov, Fiz. Tverd. Tela (Leningrad) **13**, 2357 (1971) [Sov. Phys. Solid State **13**, 1974 (1971)].
57. V. M. Gusev, K. D. Demakov, V. M. Efimov, *et al.*, Fiz. Tekh. Poluprovodn. (Leningrad) **15**, 2430 (1981) [Sov. Phys. Semicond. **15**, 1413 (1981)].
58. Yu. A. Vodakov, G. A. Lomakina, E. N. Mokhov, *et al.*, Fiz. Tekh. Poluprovodn. (Leningrad) **20**, 2153 (1986) [Sov. Phys. Semicond. **20**, 1347 (1986)].
59. Yu. M. Suleĭmanov, A. M. Grekhov, and V. M. Grekhov, Fiz. Tverd. Tela (Leningrad) **25**, 1840 (1983) [Sov. Phys. Solid State **25**, 1060 (1983)].
60. Yu. A. Vodakov, A. I. Girka, A. O. Konstantinov, *et al.*, Fiz. Tekh. Poluprovodn. (St. Petersburg) **26**, 1857 (1992) [Sov. Phys. Semicond. **26**, 1041 (1992)].
61. W. J. Choyke, in *Physics and Chemistry of Carbides, Nitrides and Borides*, Ed. by R. Freer (Kluwer, Dordrecht, 1990).
62. A. N. Andreev, M. M. Anikin, A. A. Lebedev, *et al.*, Fiz. Tekh. Poluprovodn. (St. Petersburg) **28**, 729 (1994) [Semiconductors **28**, 430 (1994)].
63. M. M. Anikin, A. S. Zubrilov, A. A. Lebedev, *et al.*, Fiz. Tekh. Poluprovodn. (Leningrad) **25**, 479 (1991) [Sov. Phys. Semicond. **25**, 289 (1991)].
64. A. A. Lebedev, V. V. Kozlovskiĭ, N. B. Strokan, *et al.*, Fiz. Tekh. Poluprovodn. (St. Petersburg) **36**, 1352 (2002) [Semiconductors **36**, 1270 (2002)].
65. B. G. Svensson, A. Hallen, M. K. Linarson, *et al.*, Mater. Sci. Forum **353–356**, 549 (2001).
66. A. Hallen, A. Henry, P. Pellegrino, *et al.*, Mater. Sci. Eng. **61–62**, 378 (1999).

67. R. K. Nadella and M. A. Capano, Appl. Phys. Lett. **70**, 886 (1997).
68. V. Nagesh, J. W. Farmer, R. F. Davis, and H. S. Kong, Appl. Phys. Lett. **50**, 1138 (1987).
69. J. McGarrity, F. McLean, M. Dealancey, *et al.*, IEEE Trans. Nucl. Sci. **39**, 1974 (1992).
70. H. Itoh, M. Yoshikawa, I. Nashiyama, *et al.*, Springer Proc. Phys. **56**, 143 (1992).
71. V. S. Vavilov, N. Yu. Isaev, B. N. Mukashev, and A. B. Spitsyn, Fiz. Tekh. Poluprovodn. (Leningrad) **6**, 1041 (1972) [Sov. Phys. Semicond. **6**, 907 (1972)].
72. Yu. V. Bulgakov and T. I. Kolomenskaya, Fiz. Tekh. Poluprovodn. (Leningrad) **1**, 422 (1967) [Sov. Phys. Semicond. **1**, 346 (1967)].
73. V. L. Vinetskiĭ and L. S. Smirnov, Fiz. Tekh. Poluprovodn. (Leningrad) **5**, 176 (1971) [Sov. Phys. Semicond. **5**, 153 (1971)].
74. D. V. Davydov, A. A. Lebedev, A. S. Tregubova, *et al.*, Mater. Sci. Forum **338–342**, 221 (2000).
75. A. O. Konstantinov, V. N. Kuz'min, L. S. Lebedev, *et al.*, Zh. Tekh. Fiz. **54**, 1622 (1984) [Sov. Phys. Tech. Phys. **29**, 949 (1984)].
76. A. O. Konstantinov, N. S. Konstantinova, O. I. Kon'kov, *et al.*, Fiz. Tekh. Poluprovodn. (St. Petersburg) **28**, 342 (1994) [Semiconductors **28**, 209 (1994)].
77. P. A. Ivanov, O. I. Kon'kov, V. N. Panteleev, and T. P. Samsonova, Fiz. Tekh. Poluprovodn. (St. Petersburg) **31**, 1404 (1997) [Semiconductors **31**, 1212 (1997)].
78. N. Atchtziger, J. Grillenberger, W. Witthuhn, *et al.*, Appl. Phys. Lett. **73**, 945 (1998).
79. H. Inui, H. Mori, and H. Fujita, Philos. Mag. B **1**, 107 (1990).
80. A. A. Lepneva, E. N. Mokhov, V. G. Oding, and A. S. Tregubova, Fiz. Tverd. Tela (Leningrad) **33**, 2217 (1991) [Sov. Phys. Solid State **33**, 1250 (1991)].
81. P. Musumeci, L. Calcagno, M. G. Grimaldi, and G. Foti, Nucl. Instrum. Methods Phys. Res. B **116**, 327 (1996).
82. A. Galeskas, J. Linnros, and P. Pirous, Appl. Phys. Lett. **81**, 883 (2002).
83. K. Kojima, T. Ohno, T. Fujimoto, *et al.*, Appl. Phys. Lett. **81**, 2974 (2002).
84. T. A. Kuhr, J. Q. Liu, H. J. Chung, *et al.*, J. Appl. Phys. **92**, 5863 (2002).
85. R. Okojie, M. Xhang, P. Pirouz, *et al.*, Appl. Phys. Lett. **79**, 3056 (2001).
86. L. J. Brillson, S. Tumakha, G. H. Jessen, *et al.*, Appl. Phys. Lett. **81**, 2785 (2002).
87. Yu. A. Vodakov, G. A. Lomakina, and E. N. Mokhov, Fiz. Tverd. Tela (Leningrad) **24**, 1377 (1982) [Sov. Phys. Solid State **24**, 780 (1982)].
88. E. Oliviero, M. L. David, M. F. Beaufort, *et al.*, J. Appl. Phys. **91**, 1179 (2002).
89. V. A. Kozlov, V. V. Kozlovskiĭ, A. N. Titkov, *et al.*, Fiz. Tekh. Poluprovodn. (St. Petersburg) **36**, 1310 (2002) [Semiconductors **36**, 1227 (2002)].
90. A. Fissel, B. Schroter, U. Kaiser, and W. Richter, Appl. Phys. Lett. **77**, 2418 (2000).
91. A. A. Lebedev, A. M. Strel'chuk, D. V. Davydov, *et al.*, Appl. Surf. Sci. **184**, 419 (2001).
92. A. A. Lebedev, A. M. Strel'chuk, N. S. Savkina, *et al.*, Pis'ma Zh. Tekh. Fiz. **28** (23), 78 (2002) [Tech. Phys. Lett. **28**, 1011 (2002)].
93. R. V. Babcock, S. L. Ruby, F. D. Schupp, and K. H. Sun, *Miniature Neutron Detectors*, Westinghouse Elec. Co. Materials Engineering Report No. 5711-6600-A (1957).
94. R. V. Babcock and H. C. Chang, in *International Atomic Energy Agency Symposium Proceedings* (1963), Vol. 1, p. 613.
95. R. V. Babcock, *Radation Damage in SiC*, Westinghouse Research and Development Center Document No. 64-8C2-432-P1 (1964).
96. V. A. Tikhomirova, O. P. Fedoseeva, and G. F. Kholuyanov, Fiz. Tekh. Poluprovodn. (Leningrad) **6**, 957 (1972) [Sov. Phys. Semicond. **6**, 831 (1972)].
97. V. A. Tikhomirova, O. P. Fedoseeva, and G. F. Kholuyanov, At. Énerg. **34** (2), 122 (1973).
98. V. A. Tikhomirova, O. P. Fedoseeva, and V. V. Bol'shakov, Izmer. Tekh., No. 6, 67 (1973).
99. A. A. Lebedev, N. S. Savkina, A. M. Ivanov, *et al.*, Fiz. Tekh. Poluprovodn. (St. Petersburg) **34**, 249 (2000) [Semiconductors **34**, 243 (2000)].
100. A. A. Lebedev, N. S. Savkina, A. M. Ivanov, *et al.*, Mater. Sci. Forum **338–342**, 1447 (2000).
101. F. Nava, P. Vanni, C. Lanzieri, and C. Canali, Nucl. Instrum. Methods Phys. Res. A **437**, 354 (1999).
102. N. B. Strokan, A. M. Ivanov, M. E. Boĭko, *et al.*, Fiz. Tekh. Poluprovodn. (St. Petersburg) **37**, 65 (2003) [Semiconductors **37**, 65 (2003)].
103. *Ion Implantation: Science and Technology*, Ed. by J. F. Ziegler (Academic, Orlando, 1984).
104. M. Rogalla, K. Runge, and A. Soldner-Rembold, Nucl. Phys. B **78**, 516 (1999).
105. R. A. Logan and A. G. Chynoweth, J. Appl. Phys. **33**, 1649 (1962).
106. V. V. Makarov, Fiz. Tekh. Poluprovodn. (Leningrad) **9**, 1098 (1975) [Sov. Phys. Semicond. **9**, 722 (1975)].
107. N. B. Strokan, Pis'ma Zh. Tekh. Fiz. **24** (5), 44 (1998) [Tech. Phys. Lett. **24**, 186 (1998)].
108. V. K. Eremin, S. G. Danengirsh, N. B. Strokan, and N. I. Tisnek, Fiz. Tekh. Poluprovodn. (Leningrad) **8**, 556 (1974) [Sov. Phys. Semicond. **8**, 355 (1974)].
109. F. Nava, P. Vanni, G. Verzellesi, *et al.*, Mater. Sci. Forum **353–356**, 757 (2001).
110. *DESSIS-6.0 Reference Manual, ISE Integrated Systems Engineering AG* (Zurich, Switzerland).
111. T. Kimoto, S. Nakazawa, K. Fujihira, *et al.*, Mater. Sci. Forum **389–393**, 165 (2002).
112. E. Kalinina, G. Kholujanov, V. Solov'ev, *et al.*, Appl. Surf. Sci. **184**, 323 (2001).
113. G. N. Violina, E. V. Kalinina, G. F. Kholuyanov, *et al.*, Fiz. Tekh. Poluprovodn. (St. Petersburg) **36**, 750 (2002) [Semiconductors **36**, 710 (2002)].
114. G. Bertuccio, R. Casigaghi, and F. Nava, IEEE Trans. Nucl. Sci. **48**, 232 (2001).
115. G. Bertuccio and R. Casigaghi, IEEE Trans. Nucl. Sci. **50**, 175 (2003).
116. CREE Research, Durham, NC 27 713, USA.

117. M. Bruzzi, F. Nava, S. Russo, *et al.*, Diamond Relat. Mater. **10**, 657 (2001).

118. P. Bergonzo, D. Tromson, C. Mer, *et al.*, Phys. Status Solidi A **185**, 167 (2001).

119. M. Rogalla, K. Runge, and A. Soldner-Rembold, Nucl. Phys. B **78**, 516 (1999).

120. R. R. Ferber and G. N. Hamilton, *Silicon Carbide High Temperature Neutron Detectors for Reactor Instrumentation*, Westinghouse Research and Development Center Document No. 65-1C2-RDFCT-P3 (1965).

121. A. R. Dulloo, F. H. Ruddy, and J. G. Seidel, *Radiation Response Testing of SiC Semiconductor Neutron Detectors for Monitoring Thermal Neutron Flux*, Westinghouse Science and Technology Report No. 97-9TK1-NUSIC-R1 (1997).

122. F. H. Ruddy, A. R. Dulloo, J. G. Seidel, *et al.*, IEEE Trans. Nucl. Sci. **45**, 536 (1998).

123. A. R. Dulloo, F. H. Ruddy, J. G. Seidel, *et al.*, IEEE Trans. Nucl. Sci. **46** (3), 275 (1999).

124. G. Lindstrom, M. Moll, and E. Fretwurst, Nucl. Instrum. Methods Phys. Res. A **426**, 1 (1999).

125. E. Verbitskaya, M. Abreu, V. Bartsch, *et al.*, IEEE Trans. Nucl. Sci. **49**, 258 (2002).

126. A. M. Ivanov, N. B. Strokan, D. V. Davydov, *et al.*, Fiz. Tekh. Poluprovodn. (St. Petersburg) **35**, 495 (2001) [Semiconductors **35**, 481 (2001)].

127. A. M. Ivanov, N. B. Strokan, D. V. Davydov, *et al.*, Appl. Surf. Sci. **184**, 431 (2001).

128. N. S. Savkina, A. A. Lebedev, D. V. Davydov, *et al.*, Mater. Sci. Eng. B **77**, 50 (2000).

129. M. M. Anikin, N. I. Kuznetsov, A. A. Lebedev, *et al.*, Fiz. Tekh. Poluprovodn. (St. Petersburg) **28**, 457 (1994) [Semiconductors **28**, 278 (1994)].

130. A. A. Lebedev, A. I. Veinger, D. V. Davydov, *et al.*, J. Appl. Phys. **88**, 6265 (2000).

131. V. V. Emtsev, T. B. Mashovets, and V. V. Mikhnovich, Fiz. Tekh. Poluprovodn. (St. Petersburg) **26**, 22 (1992) [Sov. Phys. Semicond. **26**, 12 (1992)].

132. G. Davies, Physica B (Amsterdam) **273–274**, 15 (1999).

133. V. Eremin, N. Strokan, E. Verbitskaya, and Z. Li, Nucl. Instrum. Methods Phys. Res. A **372**, 388 (1996).

134. N. B. Strokan, A. A. Lebedev, A. M. Ivanov, *et al.*, Fiz. Tekh. Poluprovodn. (St. Petersburg) **34**, 1443 (2000) [Semiconductors **34**, 1386 (2000)].

135. A. A. Lebedev, N. B. Strokan, A. M. Ivanov, *et al.*, Mater. Sci. Forum **353–356**, 763 (2001).

136. S. M. Ryvkin, Zh. Tekh. Fiz. **26**, 2667 (1956).

137. N. A. Vitovskiĭ, P. I. Maleev, and S. M. Ryvkin, Zh. Tekh. Fiz. **28**, 460 (1958) [Sov. Phys. Tech. Phys. **3**, 434 (1958)].

138. S. M. Ryvkin, *Photoelectric Effects in Semiconductors* (Fizmatgiz, Moscow, 1963; Consultants Bureau, New York, 1964).

139. A. Rose, *Concepts in Photoconductivity and Allied Problems* (Interscience, New York, 1963; Mir, Moscow, 1966).

140. A. A. Lebedev, N. B. Strokan, A. M. Ivanov, *et al.*, Appl. Phys. Lett. **79**, 4447 (2001).

141. N. B. Strokan, A. M. Ivanov, D. V. Davydov, *et al.*, Appl. Surf. Sci. **184**, 455 (2001).

142. A. A. Grinberg, Fiz. Tverd. Tela (Leningrad) **1**, 31 (1959) [Sov. Phys. Solid State **1**, 11 (1959)].

143. S. M. Sze, *Physics of Semiconductor Devices*, 2nd ed. (Wiley, New York, 1981; Mir, Moscow, 1984).

Translated by A. Spitsyn